NASA TECHNICAL MEMORANDUM

NASA TM X-62,102

NASA TM X-62,102

LARGE-SCALE WIND-TUNNEL INVESTIGATION OF A V/STOL TRANSPORT MODEL WITH PODDED LIFT FANS FORWARD AND AFT OF A LOW MOUNTED WING

Leo P. Hall and Jerry V. Kirk

Ames Research Center
Moffett Field, Calif. 94035

February 1971

INTRODUCTION

Analysis of results in references 1, 2, and 3 indicated that a configuration with outboard pod mounted front fans and rear fans located in the wing trailing-edge and fuselage juncture might have superior induced lift and variation of moment with airspeed. A large scale investigation of this type of configuration was conducted in the Ames 40- by 80-Foot Wind Tunnel.

The model used in this study was a low wing transport representative of currently operating aircraft. Two lift fans were placed in pods forward of and below the wing with the fan centerline near mid semi-span. Two rear fans were mounted at the wing trailing-edge close to the fuselage with the fan rotor in the wing chord plane.

Fan performance was measured statically and with forward speed. Longitudinal aerodynamic characteristics were obtained with the fans operating at various tip-speed ratios. Fan exit louver deflection angles were varied at each tip-speed ratio with the horizontal tail on and off. Lateral-directional characteristics were obtained at the same tip-speed ratios as the longitudinal results for zero and ten degrees angle-of-attack. Data showing the results of varying exit louver deflection for directional control and lift fan RPM for roll control were also obtained.

NOTATION

A	fan exit area, sq m (sq ft), or wing aspect ratio
b	wing span, m (ft)
c	wing chord parallel to the plane of symmetry, m (ft)
$\bar{c}$	mean aerodynamic chord, m (ft) $2/S \int_0^{b/2} c^2 dy$
C_D	drag coefficient, D/qs
C_l	rolling moment coefficient, l/qSb
C_L	lift coefficient, L/qS
C_m	pitching moment coefficient, $M/qS\bar{c}$
C_n	yawing moment coefficient, N/qSb
C_y	side-force coefficient, Y/qS
D	drag, N (lb)
D_f	diameter of the fan, m (ft)
D_e	effective fan diameter, $(\frac{4A}{\pi})^{\frac{1}{2}}$, m (ft)
i_t	horizontal-tail incidence angle, deg
l	rolling moment, m N (ft lb)
L	total lift on the model, N (lb)
M	pitching-moment, m N (ft lb)
N	yawing-moment, m N (ft lb)
P	local static pressure, N/m^2 (lb/ft^2)
P_s	free-stream static pressure, N/m^2 (lb/ft^2)
P_o	standard atmospheric pressure, N/m^2 (lb/ft^2)
q	free-stream dynamic pressure, $\rho V^2/2$ N/m^2 (lb/ft^2)

R	fan radius, m (ft)
RPM	corrected fan rotational speed, $\frac{\text{fan speed}}{\sqrt{\theta}}$
ΔRPM	difference in corrected RPM between the right and left fans
S	wing area, sq m (sq ft)
T	complete ducted thrust in the lift direction with $\alpha = 0°$ and $\beta_v = 0°$, $\rho A v_j^2$, N (lb)
v	air velocity, m/sec (ft/sec)
V_o	free-stream air velocity, m/sec (knots or ft/sec)
Y	side-force, N (lb)
α	angle of attack of the wing chord plane, deg
β	angle of sideslip, deg
β_v	fan exit vane deflection angle from [illegible] axis, deg
$\Delta\beta_v$	difference in exit vane angle between [illegible] right fans, deg
δ	relative static pressure, P_s/P_o
δ_f	trailing-edge flap deflection measured normal to the hinge line, deg
θ	ratio of ambient temperature to standard temperature (519° R)
ϵ	average downwash at the horizontal tail, deg
η	fraction of wing semi-span, 2y/b
μ	tip-speed ratio, $V_j/\omega R$
ρ	density, Kg/m^3 ($lb\text{-}sec^2/ft^4$)
ω	fan rotational speed, (radians/sec)

Subscripts

c	corrected
j	fan exit
i	induced
s	static condition
w	wing

MODEL

Photographs of the model mounted in the Ames 40- by 80-Foot Wind Tunnel are shown in figure 1. Figure 2 is a sketch of the model, propulsion system, and high lift devices with pertinent geometric details.

Fuselage.- The fuselage was circular in cross section with a maximum diameter of 1.77 meters (5.90 feet) and a length of 12.72 meters (41.71 feet).

Wing.- The low mounted wing had an aspect ratio of 5.8, taper ratio of 0.3, sweep-back of 35° at the quarter-chord line, and 6° of dihedral. An NACA 65-412 airfoil section was basic for the wing. Reference wing area used for data reduction was 21.65 square meters (233 square feet).

Propulsion system.- Four General Electric X-376 tip-turbine driven 1.1 pressure ratio lift fans, each driven by a modified T-58 gas generator, comprised the propulsion system. As shown in figure 2 the two front lift fans and the four gas generators were mounted in pods beneath the wing at approximately 50% semispan while the two rear fans were mounted with the rotor centerline in the wing chord plane, against the fuselage and near the wing trailing edge. Exit vanes, previously described in references 2, 3 and 4 were used to vector the fan exhaust for thrust during fan powered flight.

High lift devices.- A 22-percent-chord single-slotted trailing-edge flap extended from $\eta = 0.427$ to $\eta = 0.723$. The flaps were either undeflected or deflected 45° throughout the test program. An auxiliary flap was located directly behind each aft fan and was deflected to correspond with the main flap. Location and dimensions of the auxiliary

flap are shown on figure 2(a).

Leading edge slats spanned the wing except for the area taken up by the front lift fan pods (η = .38 to η = .63). The slats were deflected 20° (figure 2(b)) for the entire program.

Tail.- The horizontal tail had an aspect ratio of 2.1 with a taper ratio of 0.4. An NACA 64-009 airfoil section was used for the all moveable horizontal tail. Deflection angles of -20° to +10° were available. Only the horizontal tail was removed during tail off testing.

TESTING AND PROCEDURE

Longitudinal force and moment data were obtained for an angle of attack range of -4° to +22°. Lateral and directional characteristics were obtained at sideslip angles of -16° to +6° for 0° and 10° angle of attack. RPM was varied from 2000 to 4000 for static data (0 forward speed), for the control power data RPM was set between 2400 and 3600, for all other test points RPM was set at an average of 3300. Tunnel forward speed was varied up to a maximum of 47.3 m/sec (92.1 knots) corresponding to a Reynolds number of 6.1 million.

When angle of attack was held constant, fan speed and wind tunnel forward speed were varied independently to obtain several values of tip-speed ratio. Data were obtained at several exit vane angles with the tail on and off for both flaps deflected and undeflected. Horizontal tail effectiveness was measured and the use of differential exit vane deflection and differential fan RPM for control power was also investigated. Sideslip angle was varied at 0° and 10° angle of attack

for several tip-speed ratios.

Variable Angle of Attack Testing

When angle of attack was varied, fan RPM and forward speed were held essentially constant. Results were obtained for several tip-speed ratios at an average fan RPM of 3300. Model configurations included flap deflection, horizontal tail on or off, and front fans and/or rear fans operating.

CORRECTIONS

Power off (no fans running) force and moment data have been corrected for the effects of wind tunnel wall interference in the following manner:

$$\alpha = \alpha_u + 0.490 \; C_{L_u}$$

$$C_D = C_{D_u} + 0.0085 \; C_L^2$$

$$C_m = C_{m_u} + 0.01985 \; C_{L_u} \quad \text{(tail on only)}$$

A drag coefficient tare of 0 00765 has been subtracted from all the data to account for the lift strut and tail strut tips exposed to the free stream dynamic pressure. The power on data (lift fans operating) is presented without wind tunnel wall corrections in accordance with reference 4 which presents various ratios of model to wind tunnel size from comparison of wind tunnel and flight test results that are known to give small wall effects during power on operation. For models having concentrated lifting elements such as the model of this investigation, the most important parameter is probably the area ratio of the lifting

element. Since the area ratio of the lifting elements of this model was within the boundaries suggested, the wall corrections for the power on results are believed to be negligible.

RESULTS

The independent parameter used in the presentation of results will be lift fan tip-speed ratio unless otherwise specified. The relation between lift fan tip-speed ratio and free-stream to lift fan exit velocity ratio is shown in figure 3.

Results appear in the following order: Lift fan characteristics are presented statically and with forward speed; model longitudinal characteristics with fan operation are shown at constant angle of attack and then with variable angle of attack. Lateral-directional characteristics with sideslip angle, horizontal tail effectiveness, and the use of differential exit vane deflection and differential fan RPM for control power follow. Table 1 is an index to the figures.

Lift Fan Characteristics

Lift fan performance during static operation is shown in figure 4 for an exit vane angle of zero degrees. Each of the four lift fans was run separately and then all four were run together to give the results presented. The variation in fan thrust with forward speed as measured by equal area momentum pressure rakes mounted beneath the fan stator is shown in figure 5 for the two front fans, the two rear fans, and all four fans.

Longitudinal Characteristics at Constant Angle of Attack

Longitudinal characteristics are shown for the model at zero degrees angle of attack with exit vane deflection angles of -10° to 50° at lift fan tip-speed ratios representative of the transition from fan to wing supported flight in figures 6 through 15. Results are shown for all four fans operating with the horizontal tail on and the wing trailing edge flaps deflected 45°. With the horizontal tail removed, front fans only, rear fans only and four fans operating are shown for flap deflections of 0° and 45°. The variation in average downwash at the horizontal tail is presented in figure 15.

Longitudinal Characteristics at Variable Angle of Attack

Results are shown for an angle of attack range of -4° to 22° with power off (figure 16) and for 5 different tip-speed ratios (figure 17). At each tip speed ratio with the horizontal tail on, results are shown for the exit vane angle required to obtain thrust = drag at zero degrees angle of attack and then at exit vane deflection angles on either side of trim drag to obtain the aerodynamic derivatives. In figure 18 the horizontal tail is off and results shown are only for the drag balanced case. Results are shown in figure 19 with only the rear fans operating.

Lateral-Directional Characteristics

Lateral-directional characteristics are presented in figure 20, for an angle of sideslip range of -16° to +6° at both 0° and 10° angle of attack with power off and also for several tip-speed ratios. As with the

variable angle of attack data, the exit vanes were deflected to give thrust equal to drag at zero angle of attack and zero angle of sideslip.

Control Power

Horizontal tail effectiveness, both power off and on, is shown in figure 21. The effect of using differential exit vane deflection angles between the right and left fans for directional control is shown for 5 tip-speed ratios in figure 22. The use of differential thrust (differential fan RPM) between the right and left fans for roll control is shown in figure 23 for the same tip-speed ratio range as shown in figure 22.

REFERENCES

1. Kirk, Jerry V.; Hodder, Brent K.; and Hall, Leo P.: Large-Scale Wind-Tunnel Investigation of a V/STOL Transport Model with Wing-Mounted Lift Fans and Fuselage-Mounted Lift-Cruise Engines for Propulsion. NASA TN D-4233, 1967.

2. Hall, Leo P.; Hickey, David H.; and Kirk, Jerry V.: Aerodynamic Characteristics of a Large-Scale V/STOL Transport Model with Lift and Lift-Cruise Fans. NASA TN D-4092, 1967.

3. Dickinson, Stanley O.; Hall, Leo P.; and Hodder, Brent K.: Aerodynamic Characteristics of a Large-Scale V/STOL Transport Model with Tandem Lift Fans Mounted at Mid-Semispan of the Wing. NASA TN D-6234, 1971.

4. Cook, Woodrow L.; and Hickey, David H.: Comparison of Wind-Tunnel and Flight-Test Aerodynamic Data in the Transition Flight Speed Range for Five V/STOL Aircraft. Paper 26, NASA SP-116, 1966.

TABLE I.- LIST OF FIGURES

FIGURE	α, DEG.	β, DEG.	FANS OPERATING	λ_J	β_V, DEG.	i_T, DEG.	δ_F, DEG	δ_{FAUX}, DEG	REMARKS
FAN CHARACTERISTICS									
3	0	0	FRONT, REAR, ALL 4	VARIABLE	0	0	0	0	VELOCITY RATIO VERSUS TIP SPEED RATIO
4			SINGLY, ALL 4	0			45		STATIC THRUST DATA
5			FRONT, REAR, ALL 4	VARIABLE			45		
LONGITUDINAL CHARACTERISTICS AT ZERO ANGLE OF ATTACK									
6	0	0	ALL 4	VARIABLE	VARIABLE	0	45	0	C_L, C_D & C_M VERSUS TIP SPEED RATIO
7			ALL 4			0	45	45	
8			FRONT			OFF	0	0	
9			REAR						
10			ALL 4						
11			FRONT				45	45	
12			REAR						
13			ALL 4						
14			ALL 4						CIRCULAR INLET GUIDE VANE INSTALLED
15			ALL 4			N/A			DOWNWASH AT THE HORIZONTAL TAIL
LONGITUDINAL CHARACTERISTICS WITH VARIABLE ANGLE OF ATTACK									
16	VARIABLE	0	NONE	N/A	90	0 & OFF	0 & 45	0 & 45	POWER OFF DATA
17(a)			ALL 4	0.09	-10, 2, 12 & 22				
17(b)				0.12	-10, 5, 15 & 25				

TABLE I. - CONTINUED

FIGURE	α, deg.	β, deg.	FANS OPERATING	μ	β_V, deg.	i_T, deg.	δ_F, deg	$\delta_{F\,AUX}$, deg	REMARKS
17(c)	VARIABLE	0	ALL 4	0.19	-10, 0, 13, 23, 33	0	45	45	LONGITUDINAL CHARACTERISTICS WITH VARIABLE ANGLE OF ATTACK. - CONTINUED
17(d)	↓	↓	↓	0.24	-10, 10, 24, 34, 40	↓	↓	↓	
17(e)	↓	↓	↓	0.31	-10, 10 30, 40	↓	↓	↓	
18(a)	VARIABLE	0	ALL 4	0.09	12	OFF	45	45	
18(b)	↓	↓	↓	0.13	15	↓	↓	↓	
18(c)	↓	↓	↓	0.19, 0.25	23, 34	↓	↓	↓	
19(a)	VARIABLE	0	REAR	0.09	12	OFF	45	45	
19(b)	↓	↓	↓	0.12, 0.19 0.25	15, 23, 34	↓	↓	↓	
LATERAL - DIRECTIONAL CHARACTERISTICS									
20(a)	0, 10	VARIABLE	NONE	N/A	90	0	45	45	POWER OFF
20(b)	0, 10	↓	ALL 4	0.09	12	↓	↓	↓	
20(c)	0, 10	↓	↓	0.12	15	↓	↓	↓	
20(d)	0, 10	↓	↓	0.19	23	↓	↓	↓	
20(e)	0, 10	↓	↓	0.25	34	↓	↓	↓	
20(f)	0, 10	↓	↓	0.31	40	↓	↓	↓	
21(a)	0, 10	0	NONE	N/A	90	VARIABLE	45	45	POWER OFF
21(b)	0	0	ALL 4	0.18, 0.25, 0.31	23, 34, 40	↓	↓	↓	

TABLE I. - CONCLUDED

FIGURE	α, deg.	β, deg.	FANS OPERATING	μ	β_V, deg.	i_T, deg.	δ_E, deg.	$\delta_{E\,AUX}$, deg.	REMARKS
LATERAL-DIRECTIONAL CONTROL POWER									
22	0	0	ALL 4	0.09, 0.12, 0.18, 0.25, 0.31	VARIABLE	0	45	45	DIRECTIONAL CONTROL
23	0	0	ALL 4	0.09, 0.12, 0.18, 0.24, 0.30	12, 15, 23, 34, 40	0	45	45	ROLL CONTROL

(a) Top view.

Figure 1.- Photographs of the model mounted in the Ames 40- by 80-Foot Wind Tunnel.

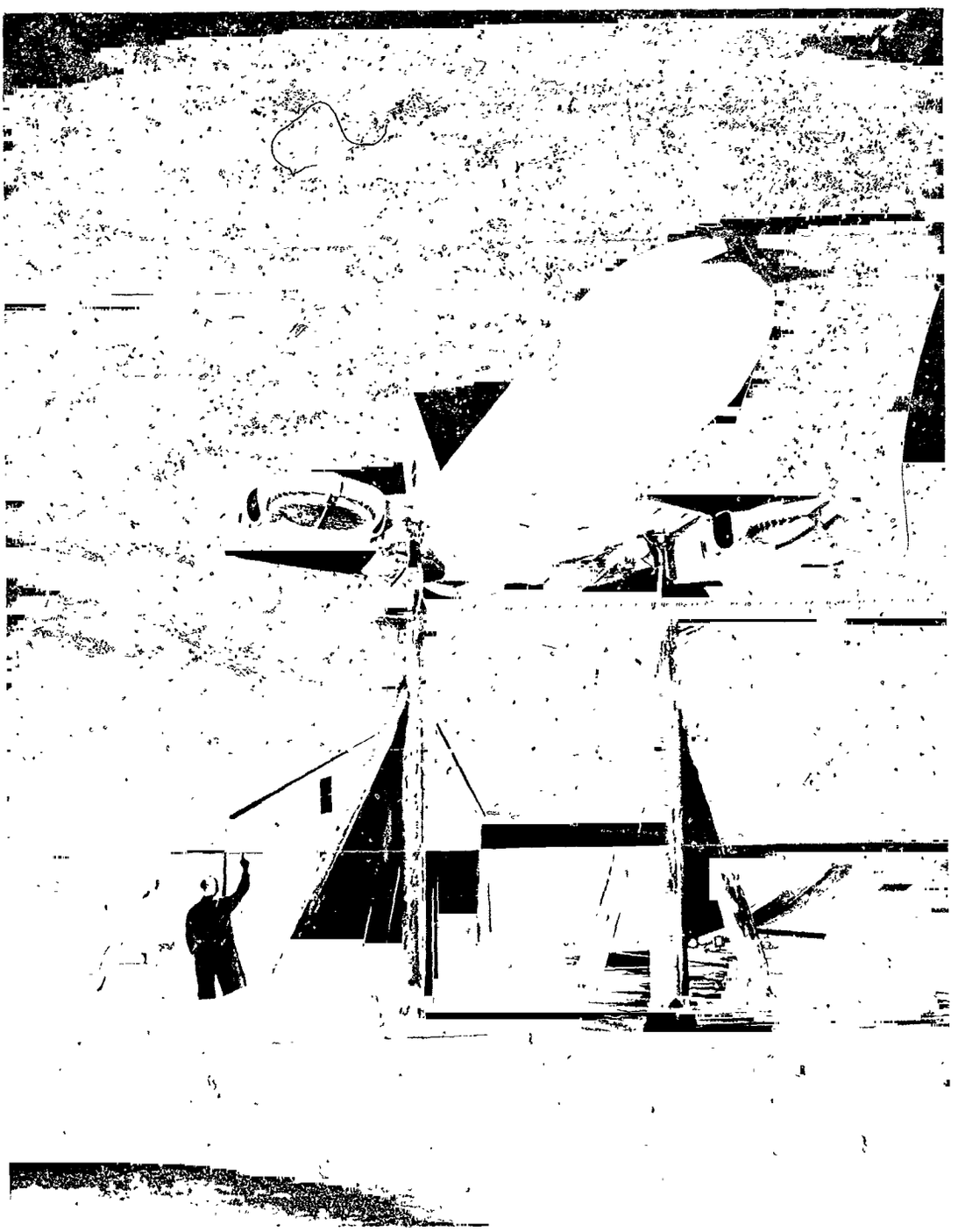

(b) 3/4 front view.

Figure 1.- Concluded.

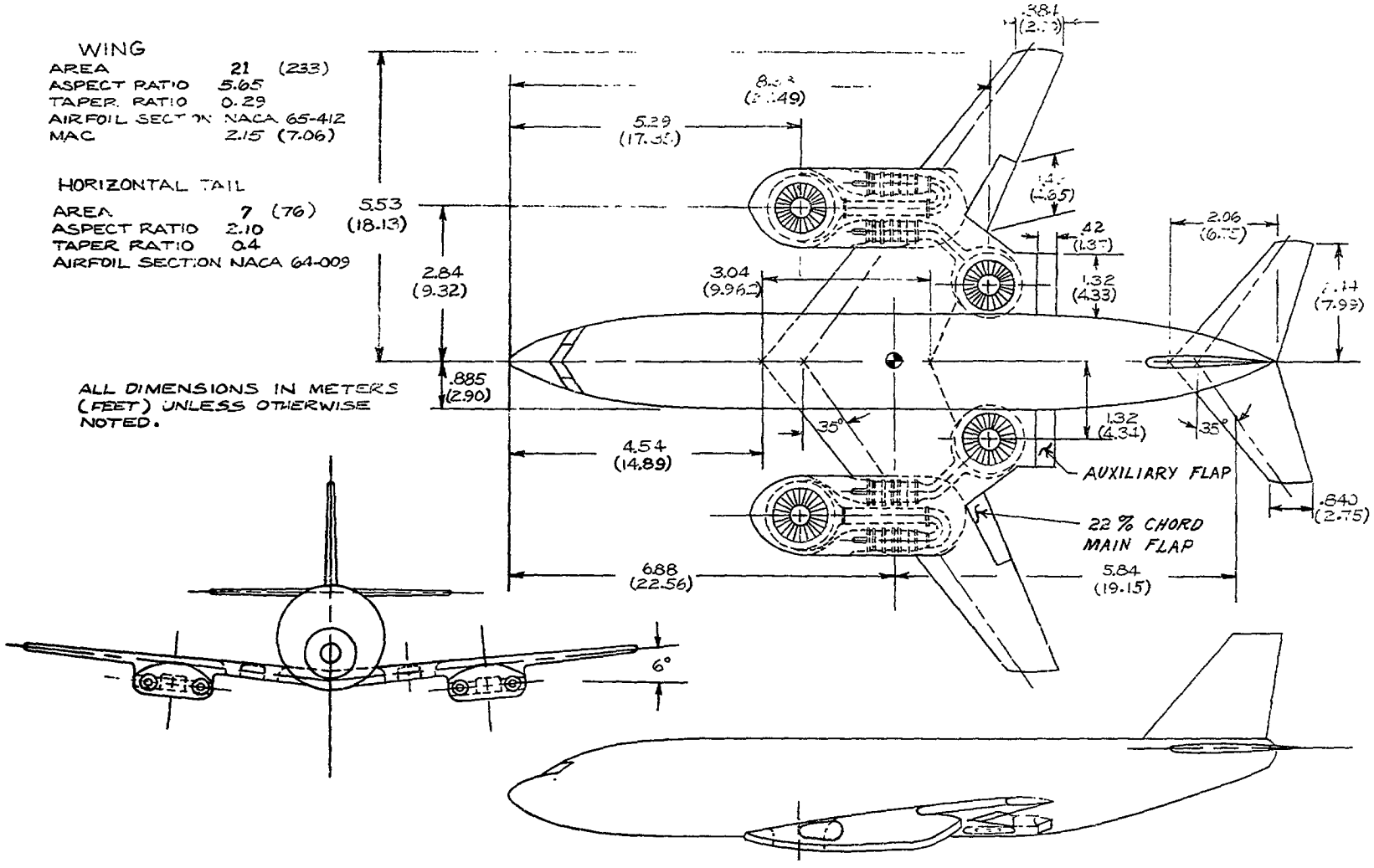

(a) Geometric details.

Figure 2.- General arrangement of the lift fan transport model.

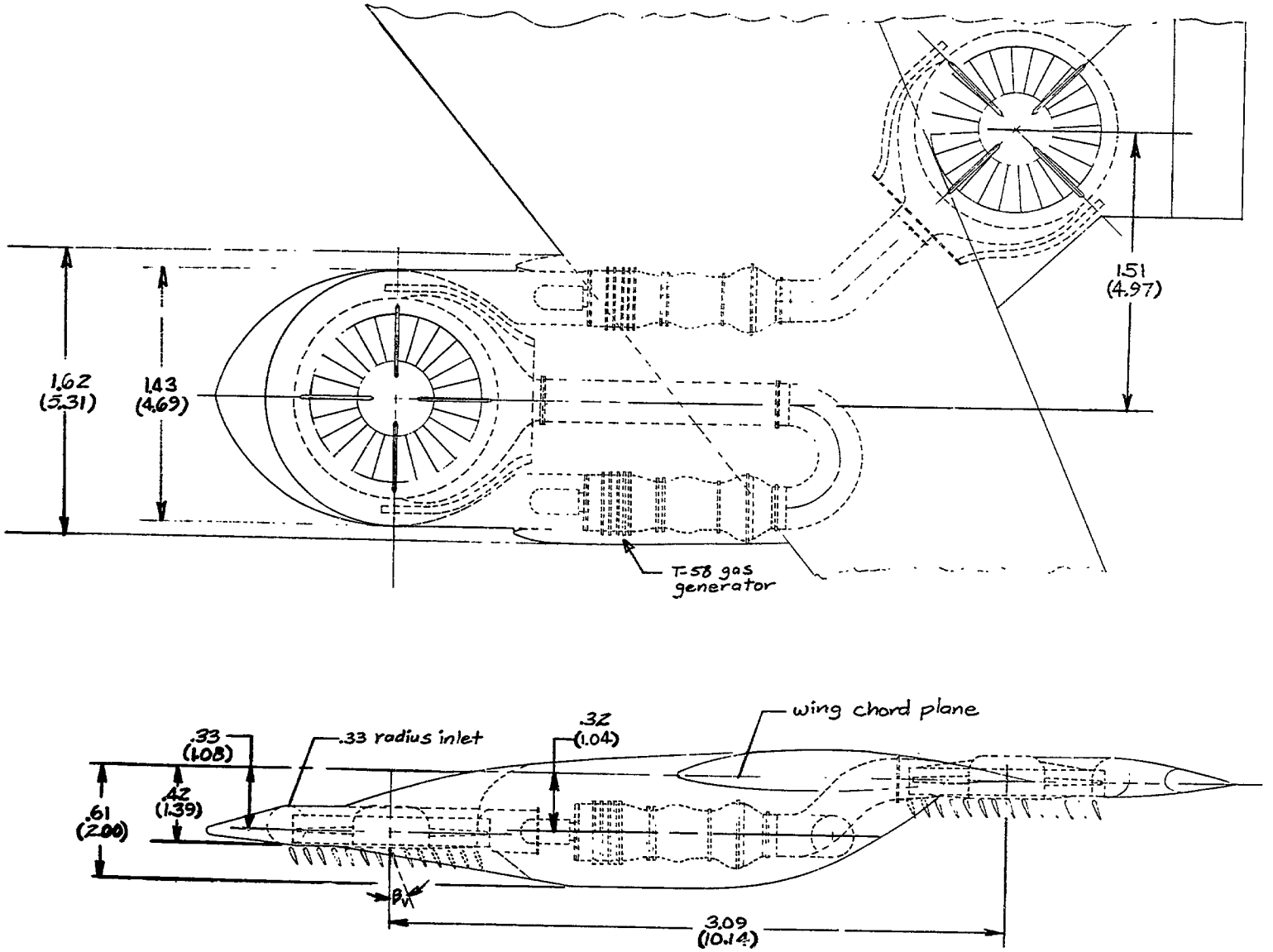

(b) Details of the fans and gas generators.

Figure 2.- Continued.

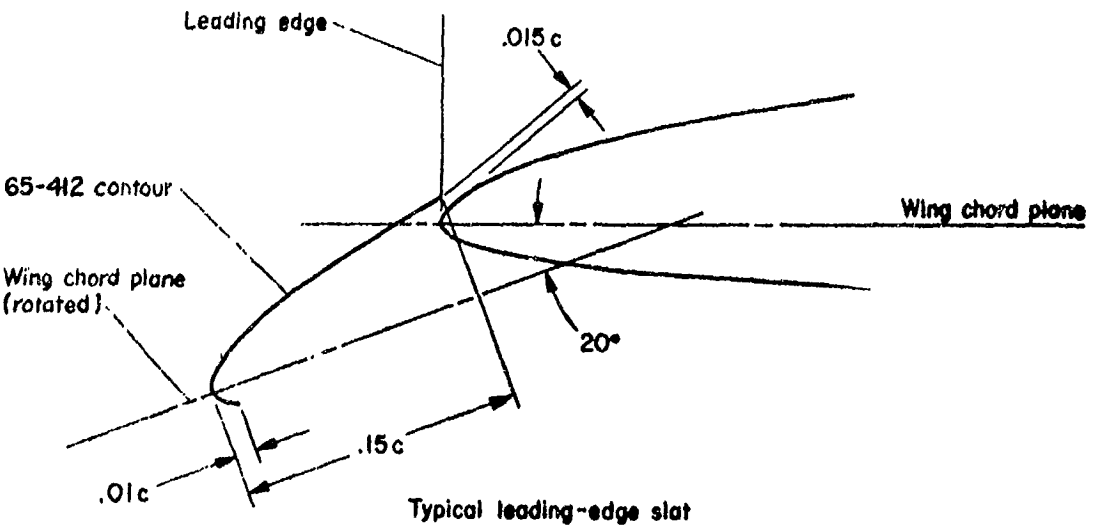

Typical leading-edge slat

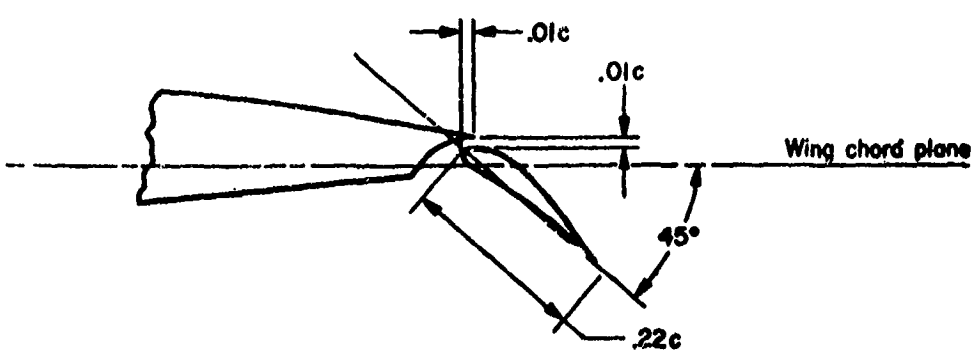

Typical trailing-edge flap

(c) Details of the leading edge slat and trailing edge flap.

Figure 2.- Concluded.

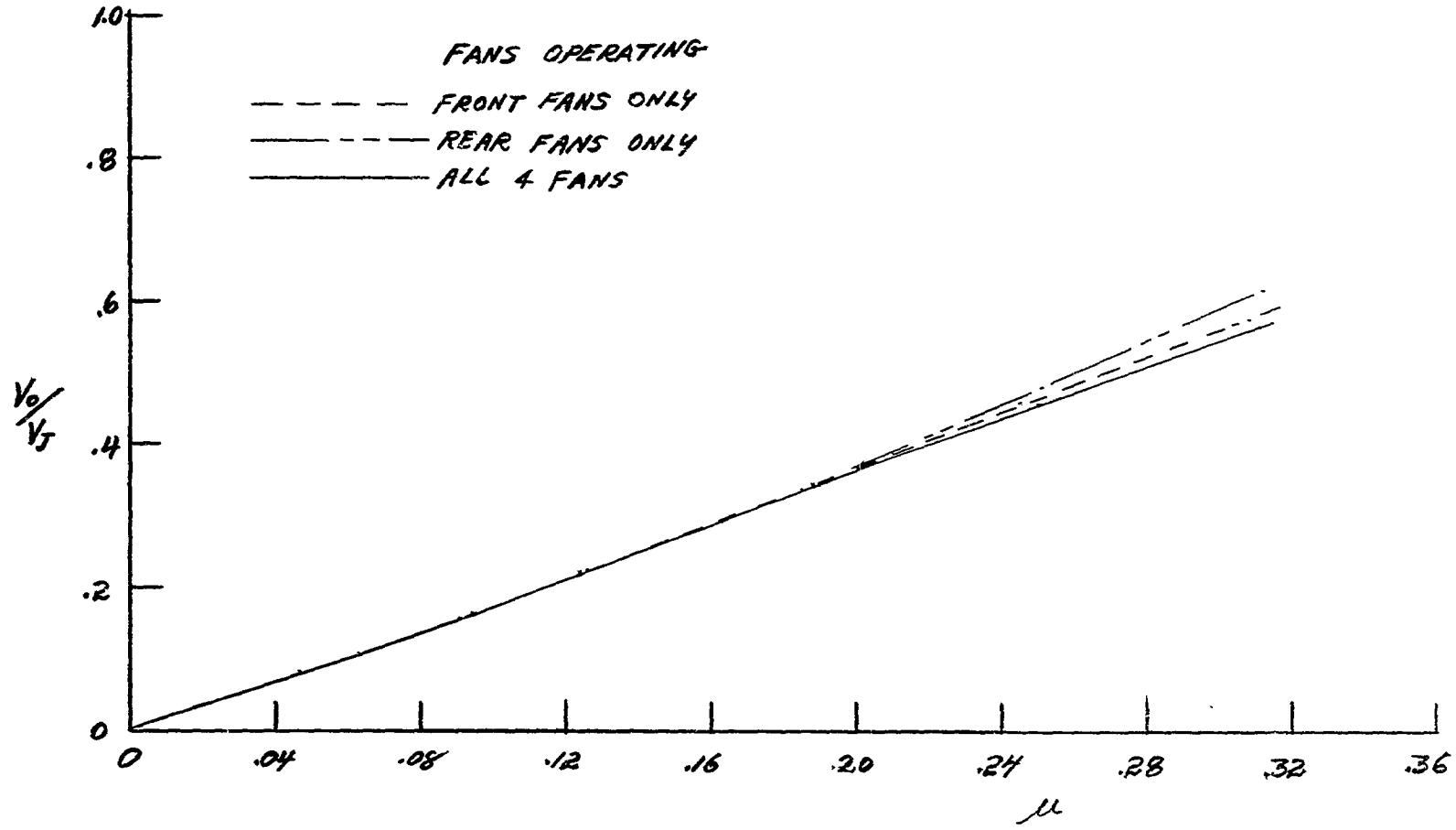

Figure 3.- The variation in average velocity ratio with tip speed ratio; $\alpha = 0^0$, $\beta_v = 0^o$, $\delta_f = 0^o$.

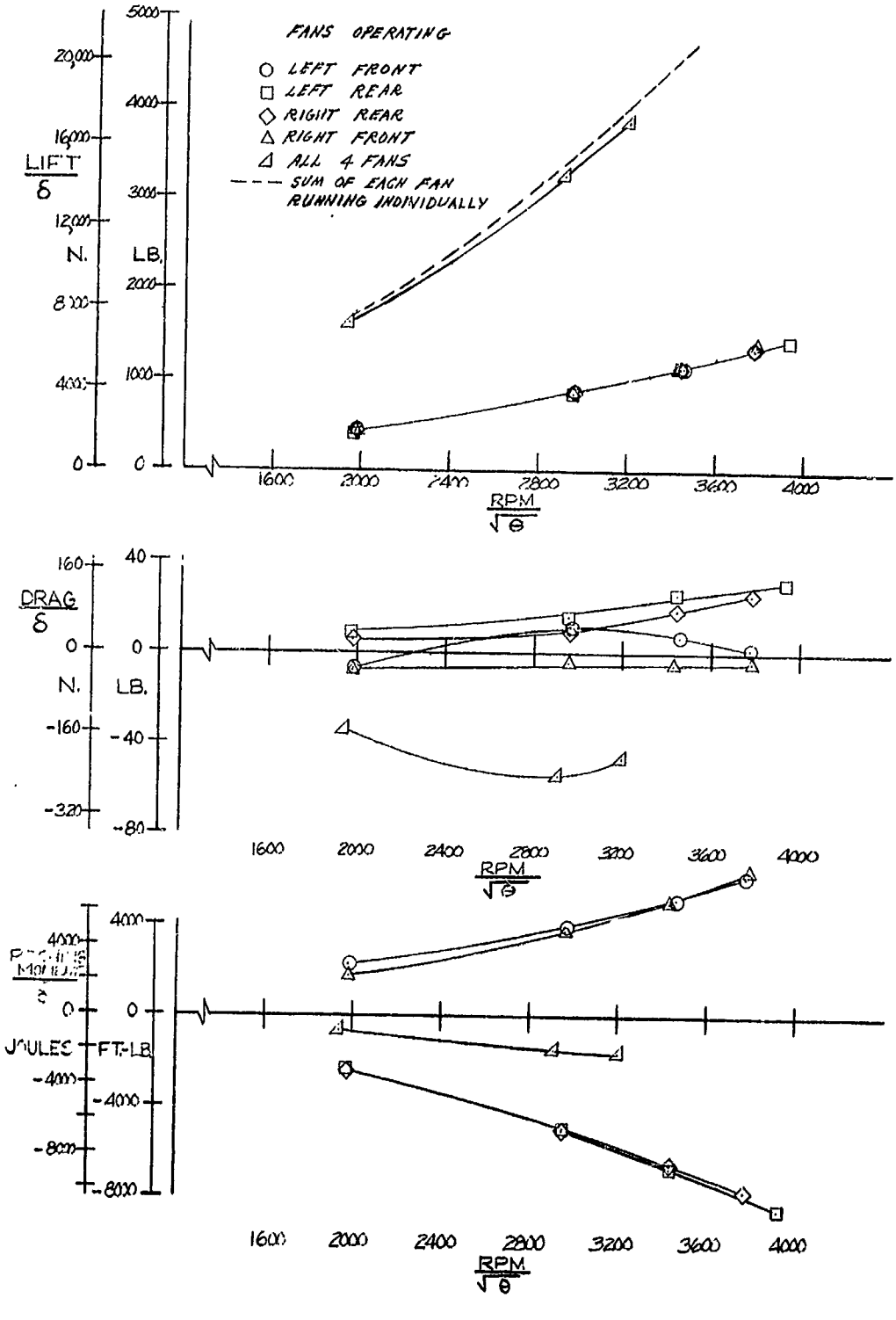

Figure 4.- Zero airspeed characteristics with fan operation; $i_t = 0^o$, $\beta_v = 0^o$, $\delta_f = 45^o$, $\delta_{f_{aux}} = 0^o$.

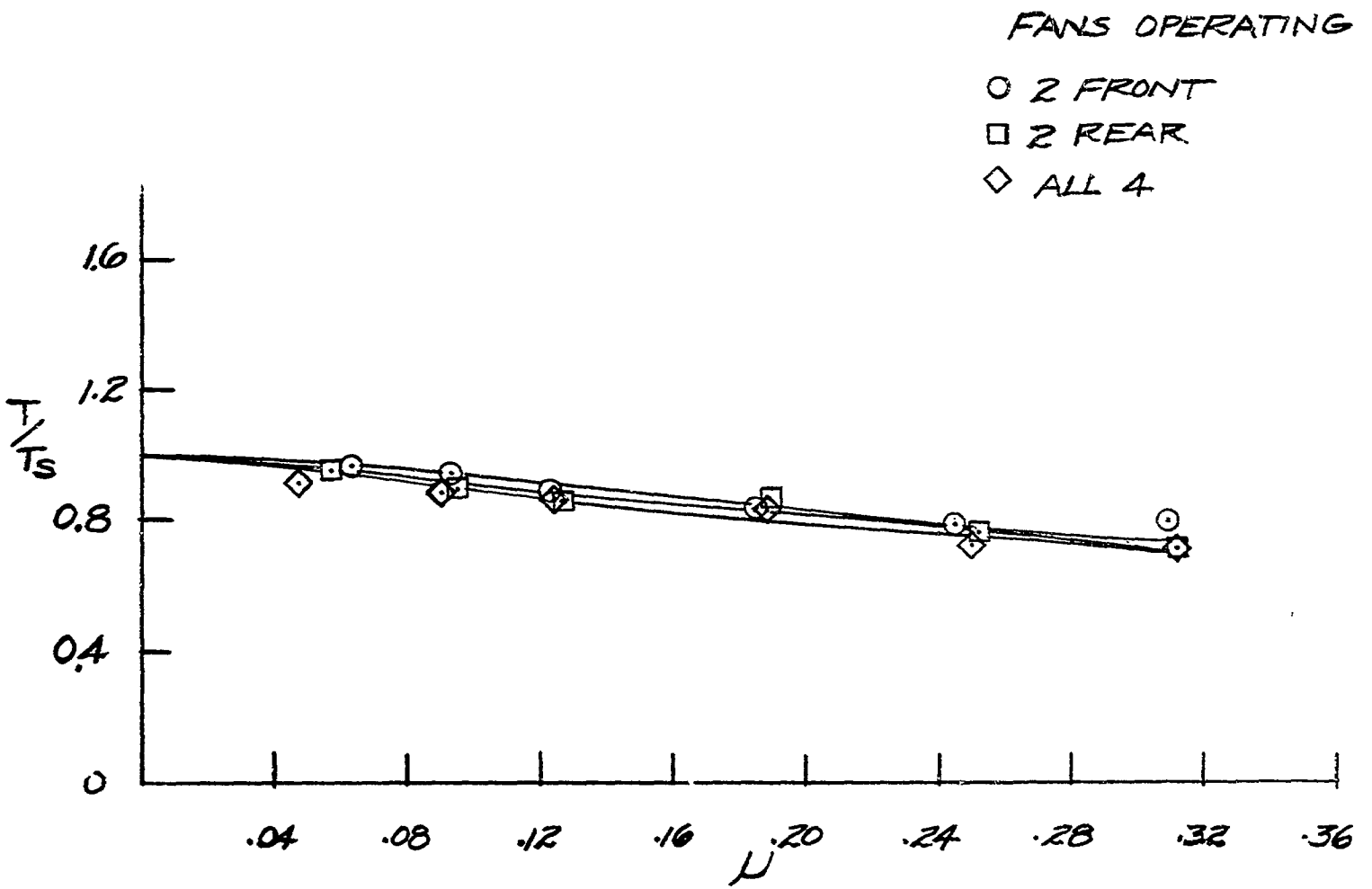

Figure 5.- The effect of forward speed (tip speed ratio) on average fan thrust; $\alpha = 0^{o}$, $\beta_{v} = 0^{o}$.

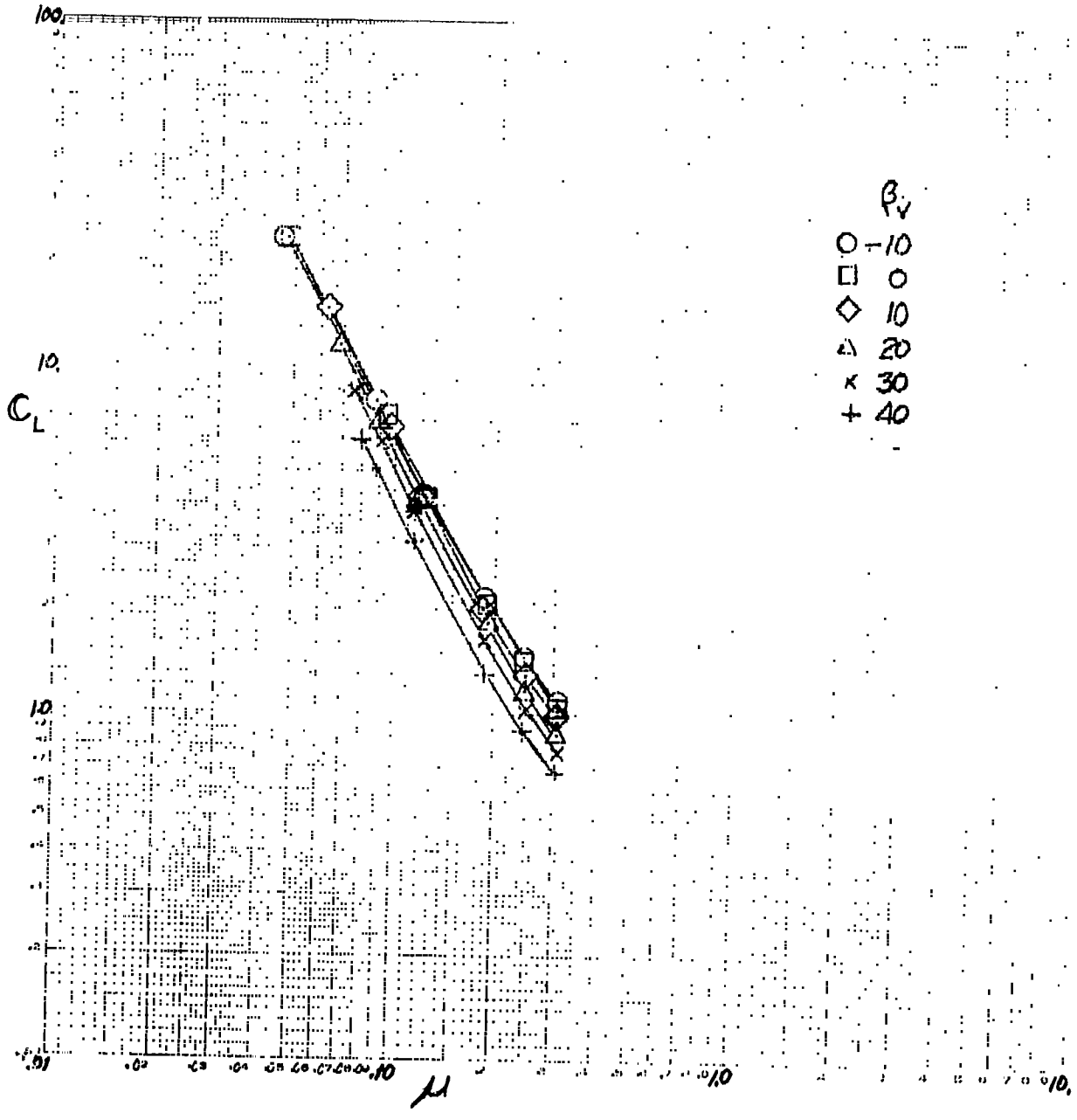

(a) C_L vs μ.

Figure 6.- The effect of tip speed ratio on longitudinal characteristics; 4 fans operating, RPM = 3300, $i_t = 0^o$, $\delta_f = 45^o$, $\delta_{f_{aux}} = 0^o$.

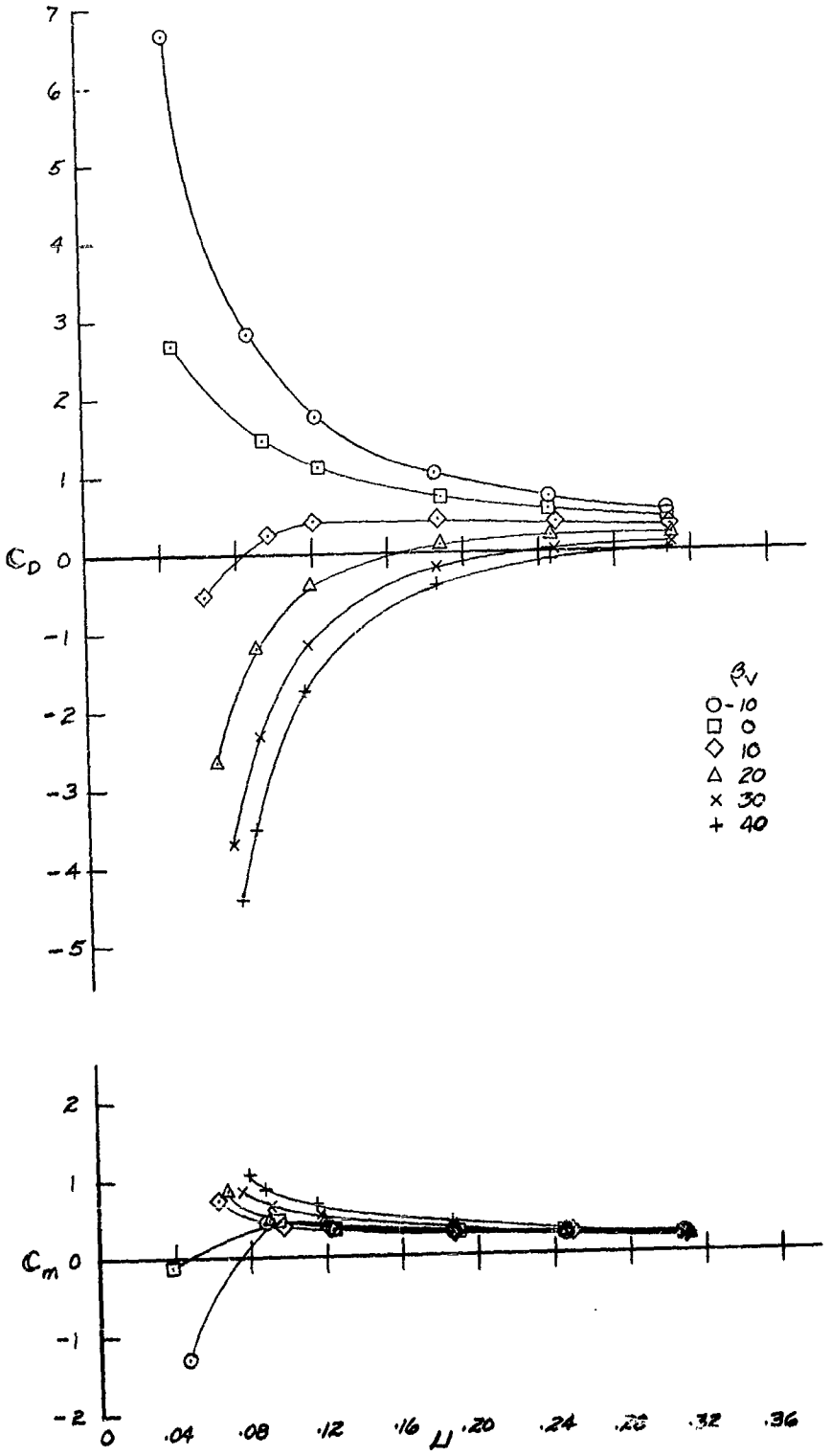

(b) C_D, C_m, vs μ.

Figure 6.- Concluded.

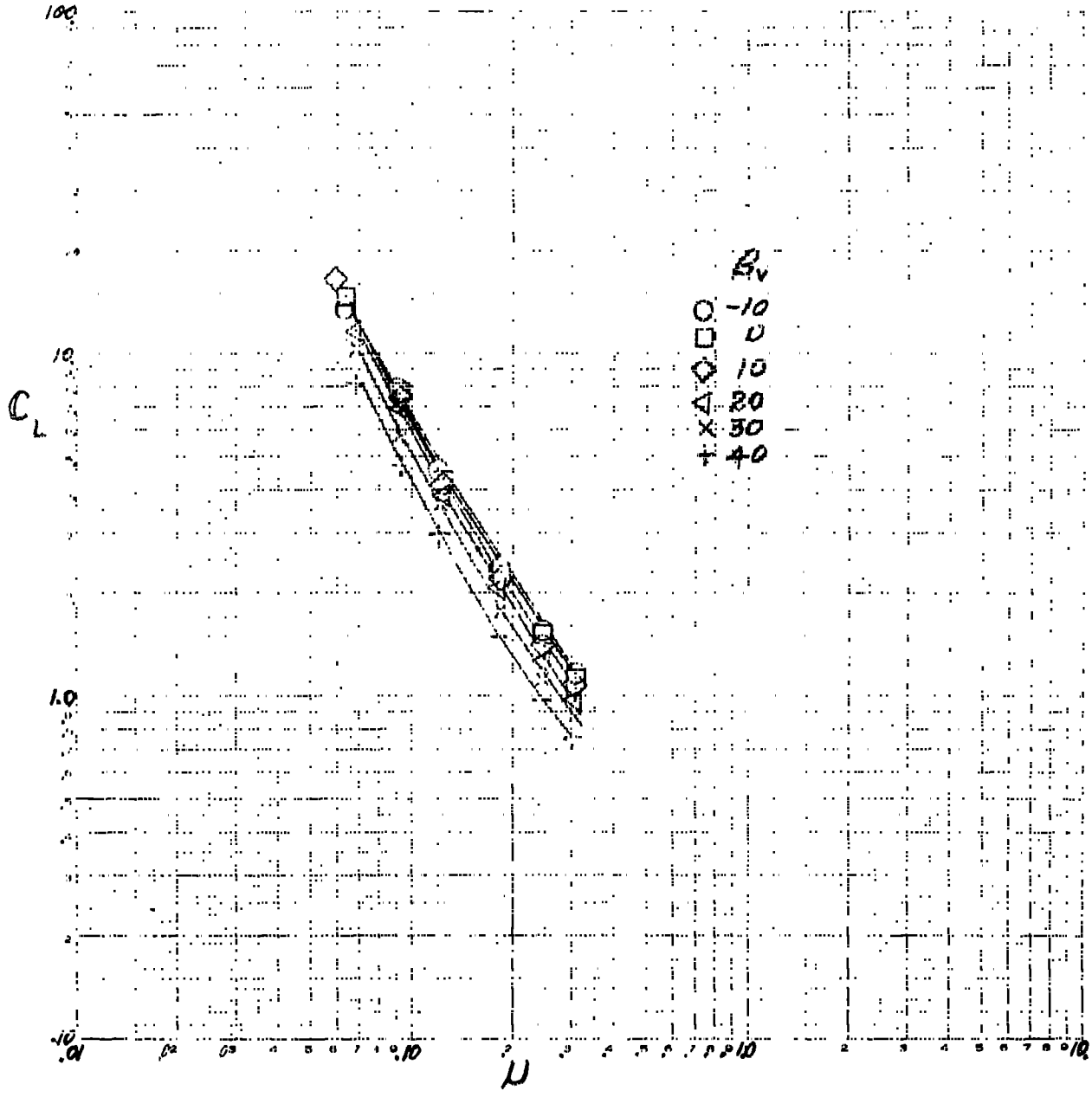

(a) C_L vs μ.

Figure 7.- The effect of tip speed ratio on longitudinal characteristics; 4 fans operating, RPM = 3300, $i_t = 0^o$, $\delta_f = 45^o$, $\delta_{f_{aux}} = 45^o$.

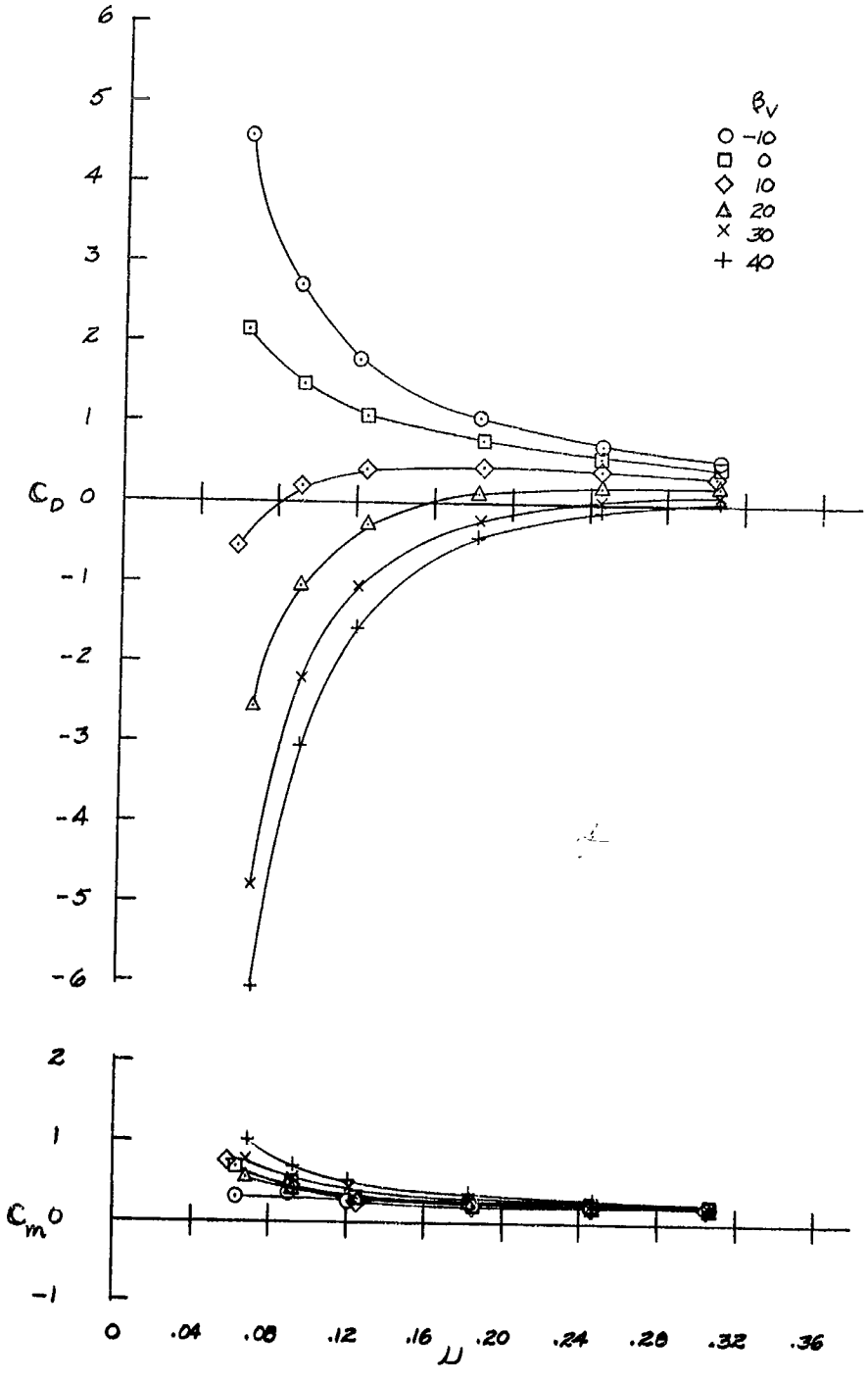

(b) C_D, C_m, vs μ.

Figure 7.- Concluded.

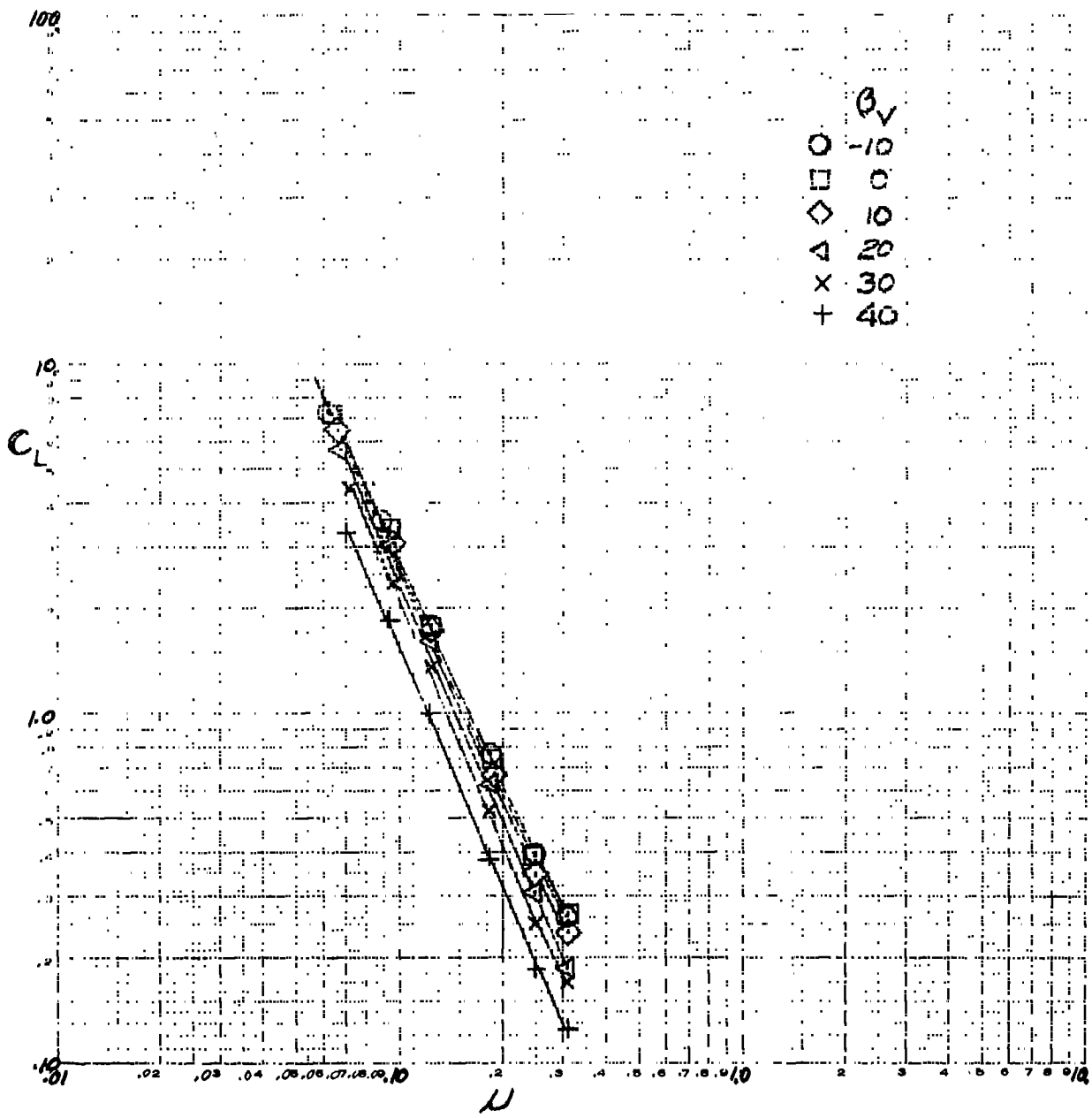

(a) C_L vs μ.

Figure 8.- The effect of tip speed ratio on longitudinal characteristics; front fans operating, RPM = 3300, tail off, $\delta_f = 0^\circ$, $\delta_{f_{aux}} = 0^\circ$.

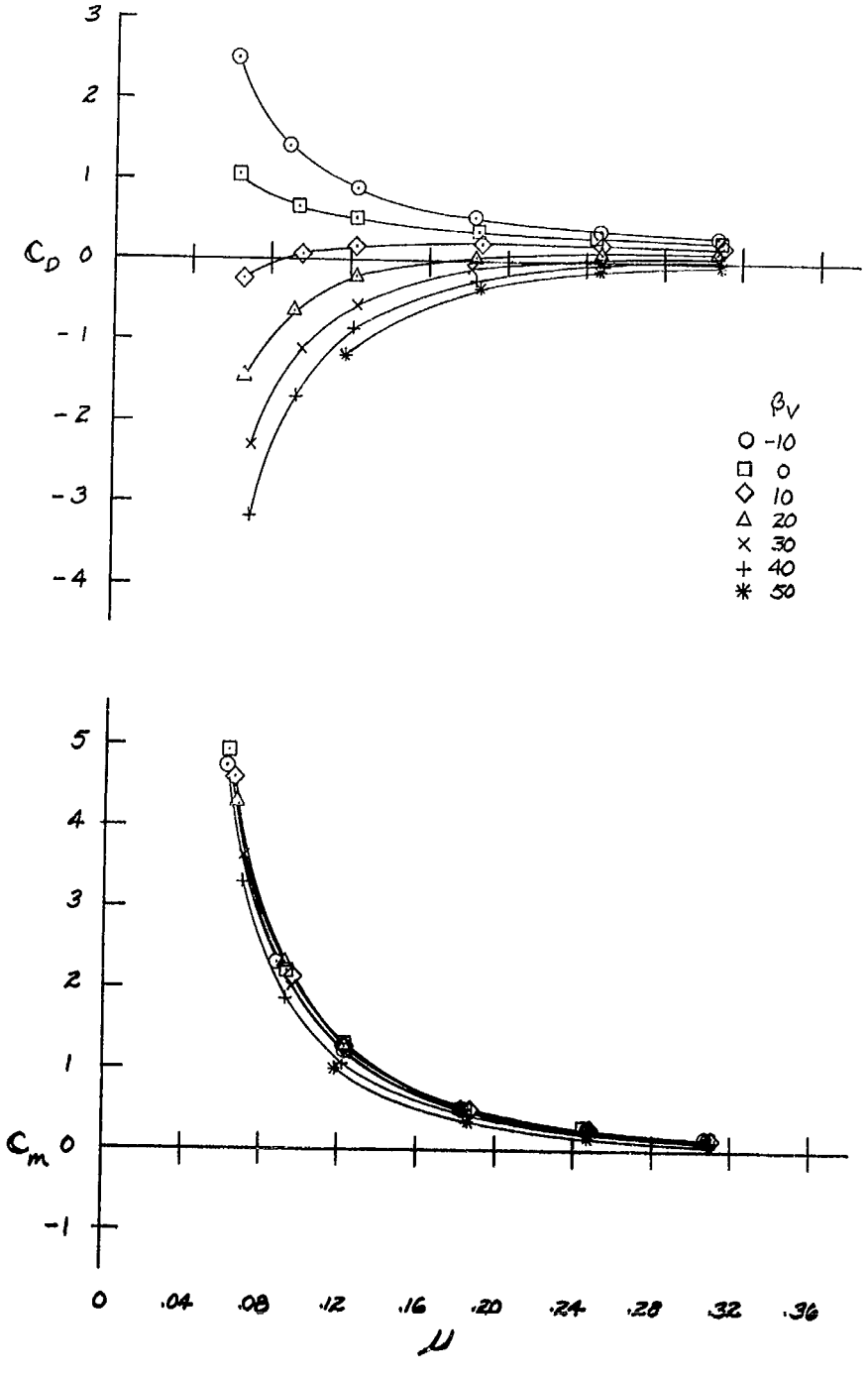

(b) C_D, C_m, vs μ.

Figure 8.- Concluded.

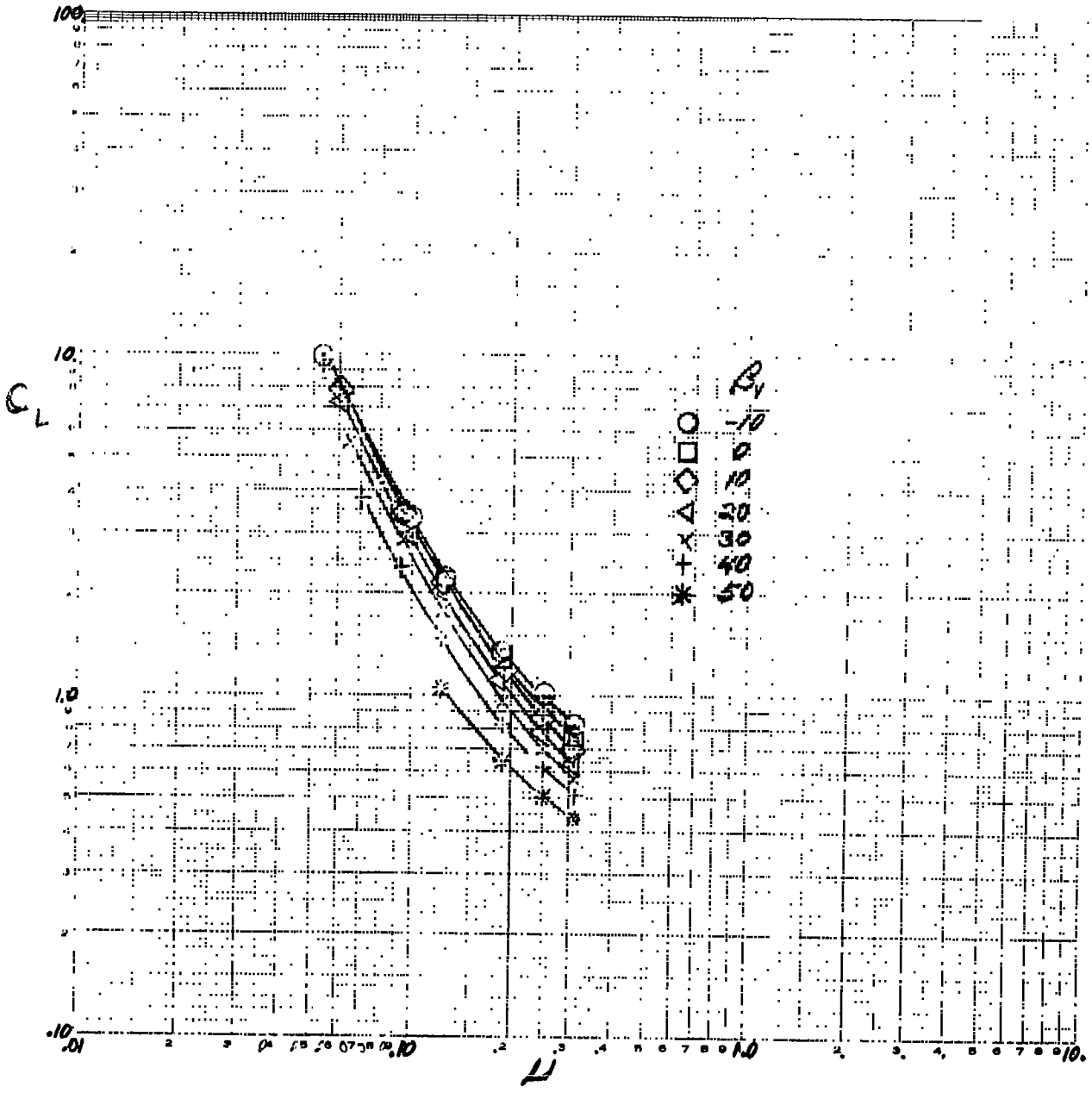

(a) C_L vs μ.

Figure 9.- The effect of tip speed ratio on longitudinal characteristics; rear fans operating, RPM = 3300, tail off, $\delta_f = 0^o$, $\delta_{f_{aux}} = 0^o$.

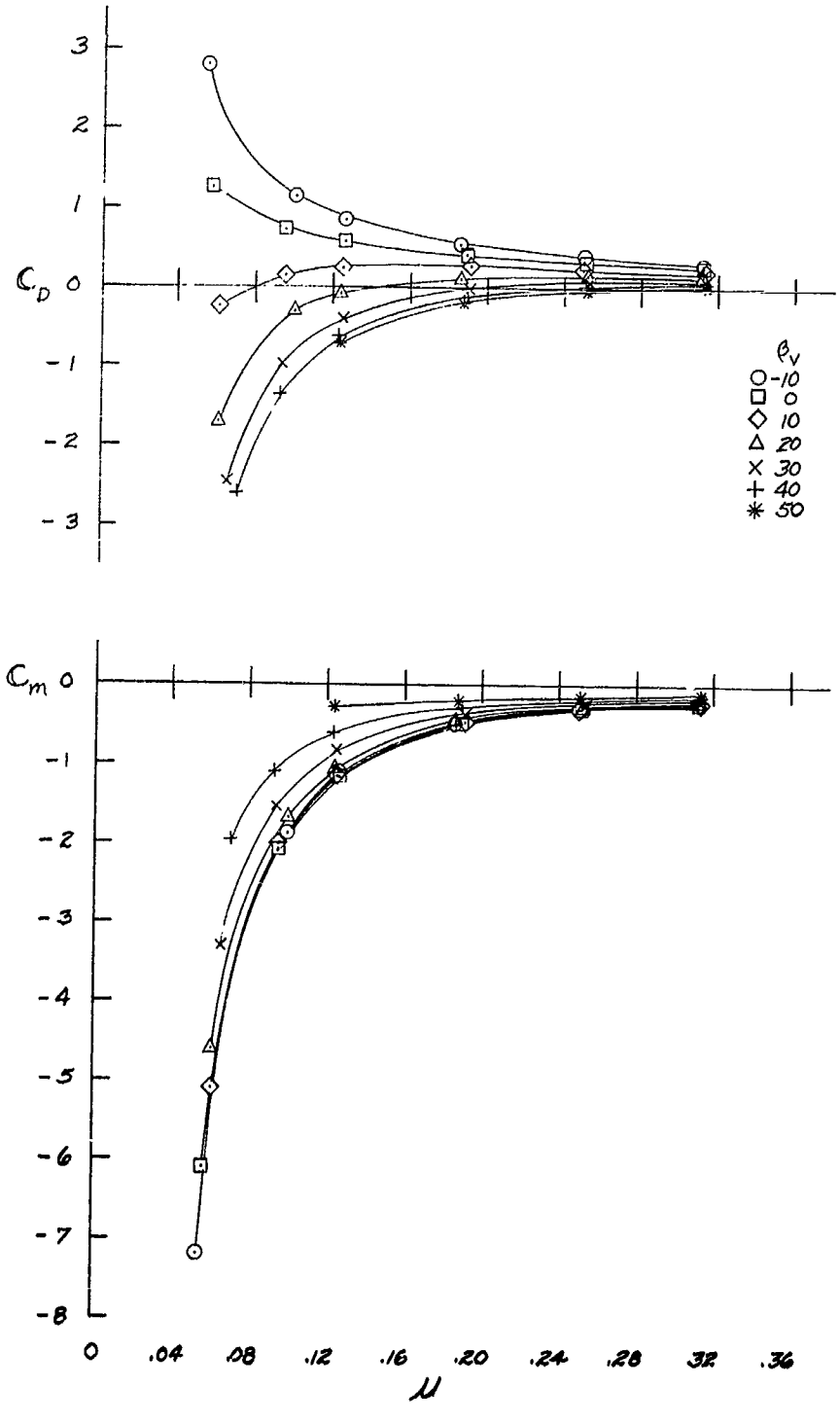

(b.) C_D, C_m, vs μ.

Figure 9.- Concluded.

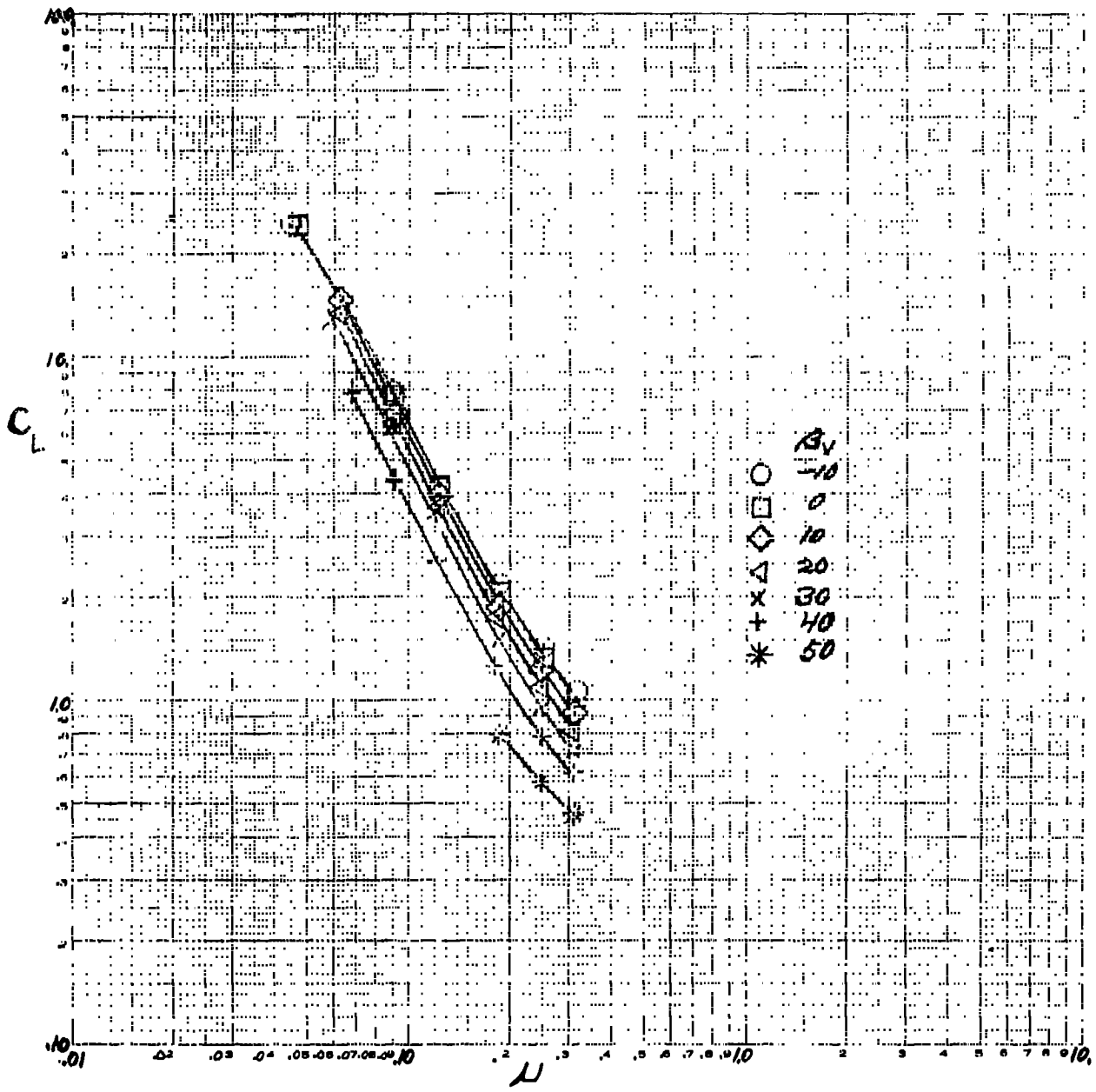

(a) C_L vs μ.

Figure 10.- The effect of tip speed ratio on longitudinal characteristics; 4 fans operating, RPM = 3300, tail off, $\delta_f = 0^\circ$, $\delta_{f_{aux}} = 0^\circ$.

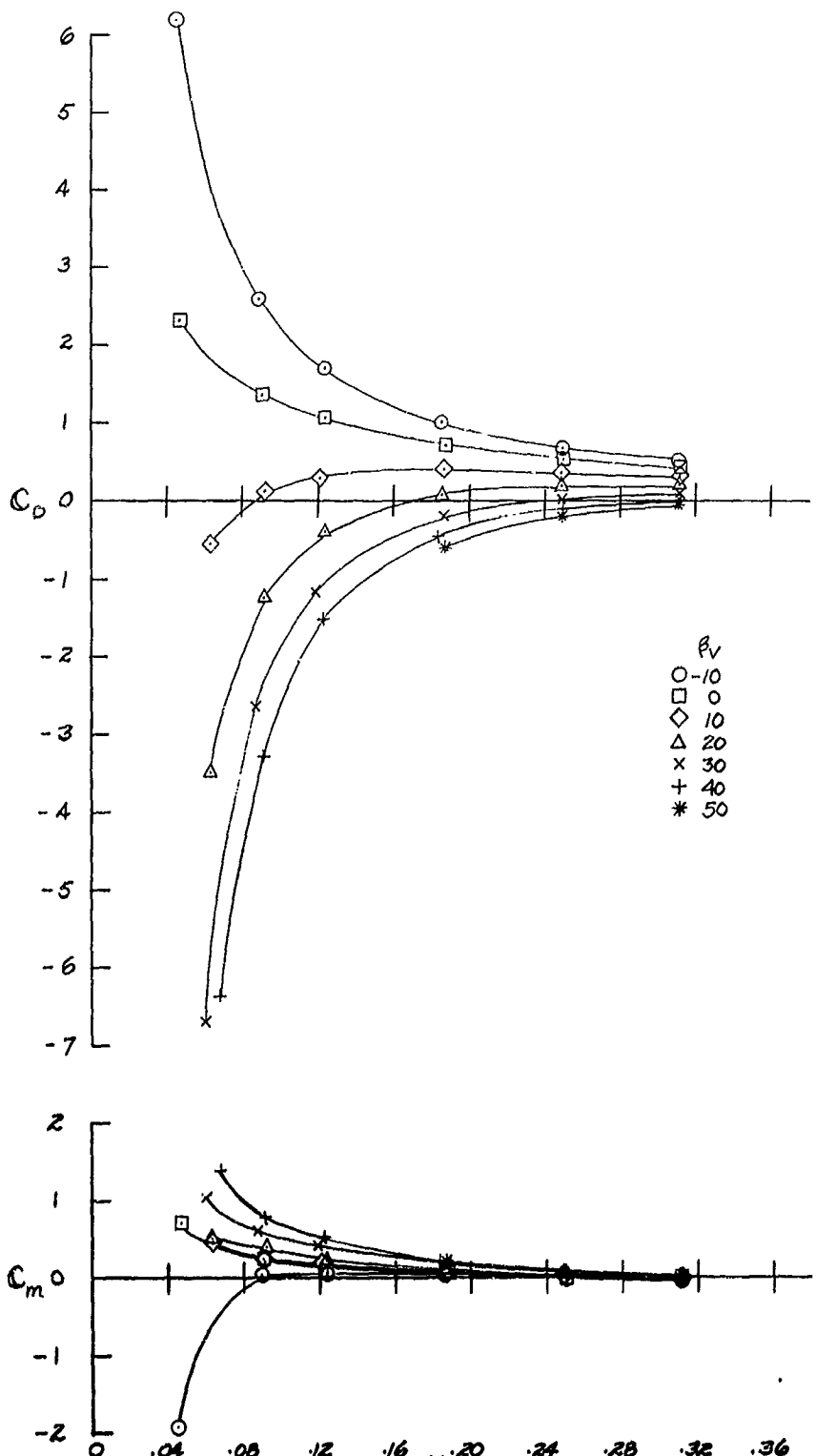

(b) C_D, C_m vs μ.

Figure 10.- Concluded.

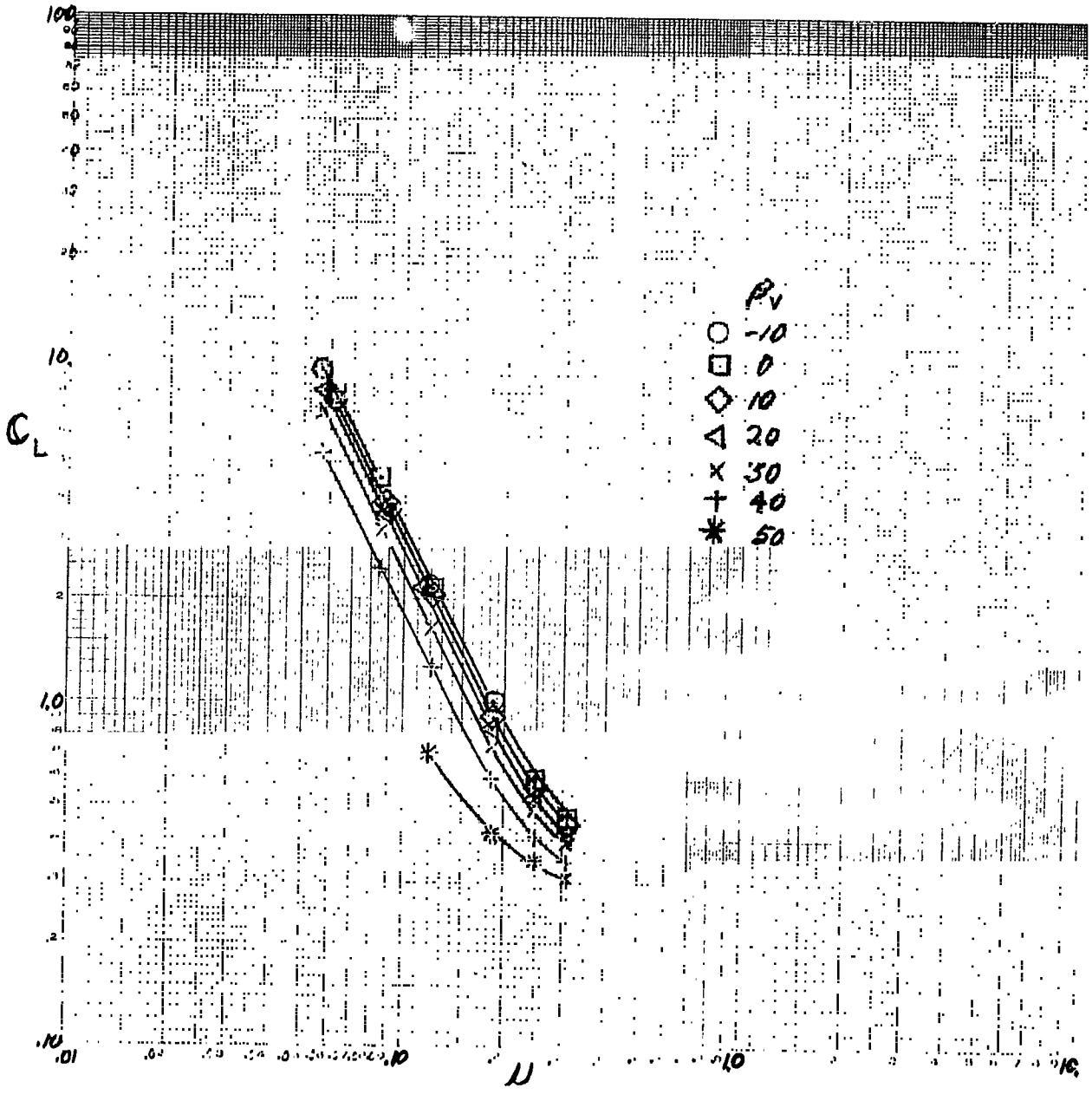

(a) C_L vs μ.

Figure 11.- The effect of tip speed ratio on longitudinal characteristics; front fans operating, RPM = 3300, tail off, $\delta_f = 45^\circ$, $\delta_{f_{aux}} = 45^\circ$.

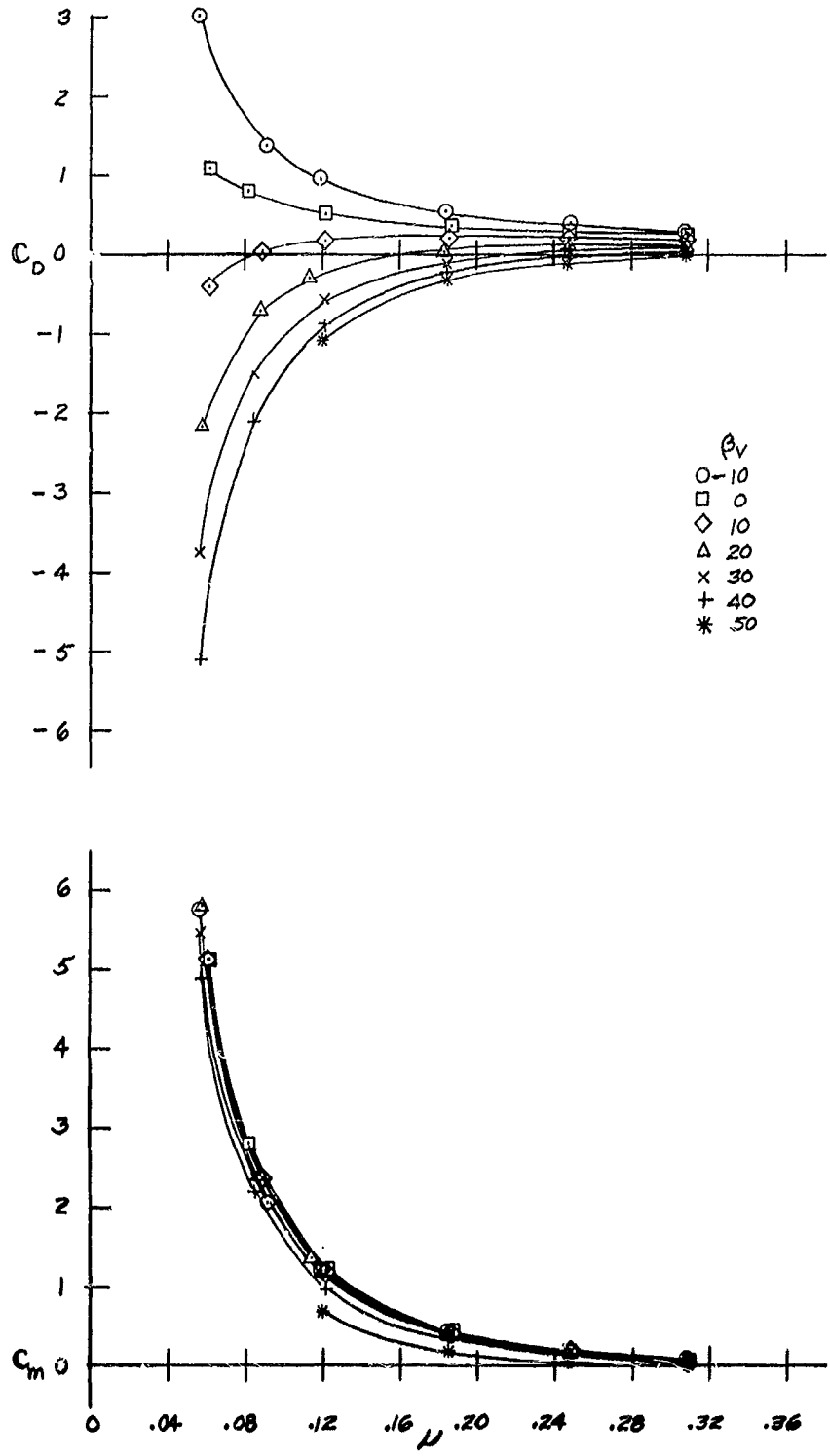

(b) C_D, C_m vs μ.

Figure 11.- Concluded.

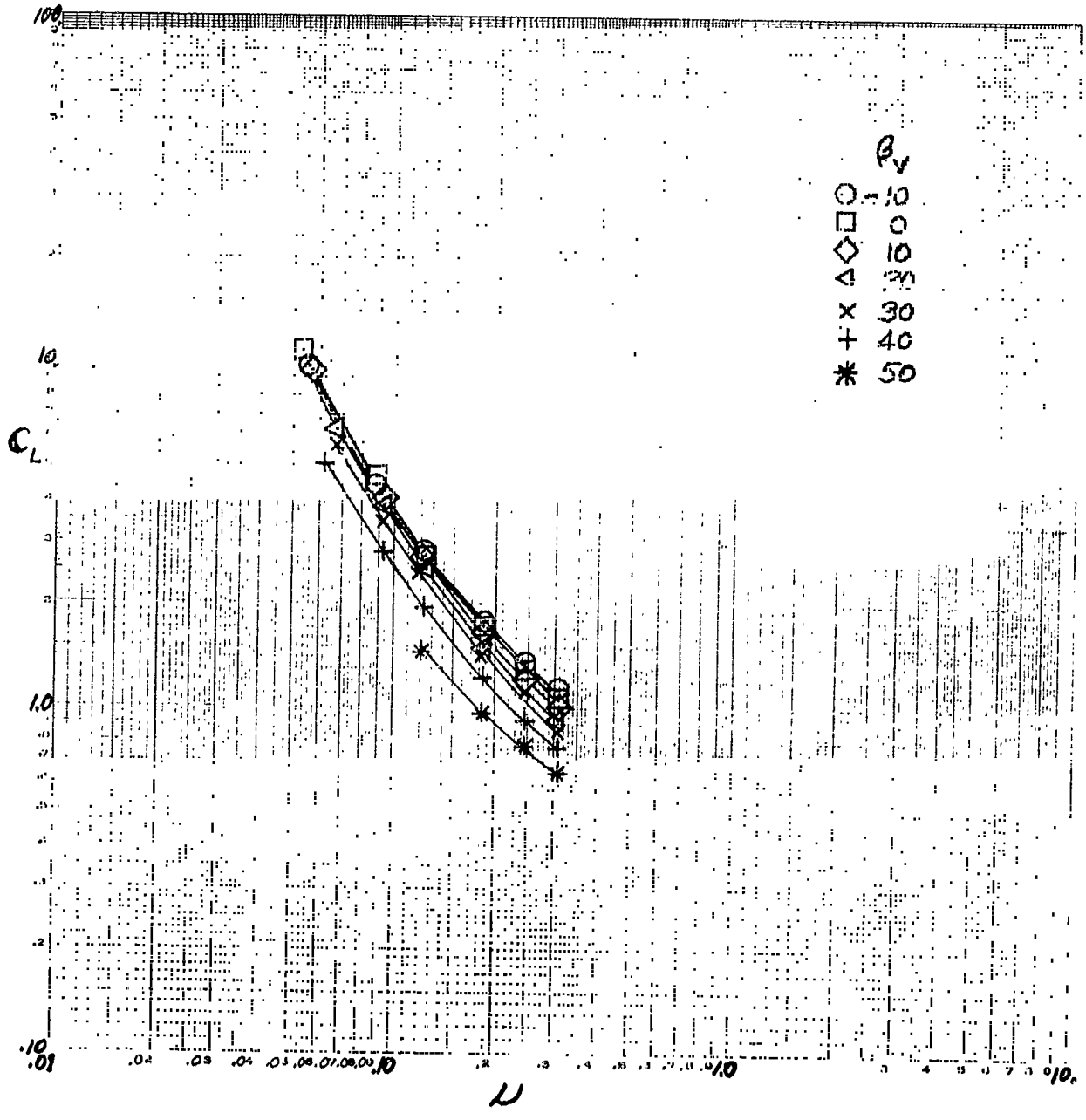

(a) C_L vs μ.

Figure 12.- The effect of tip speed ratio on longitudinal characteristics; rear fans operating, RPM = 3300, tail off, $\delta_f = 45^\circ$, $\delta_{f_{aux}} = 45^\circ$.

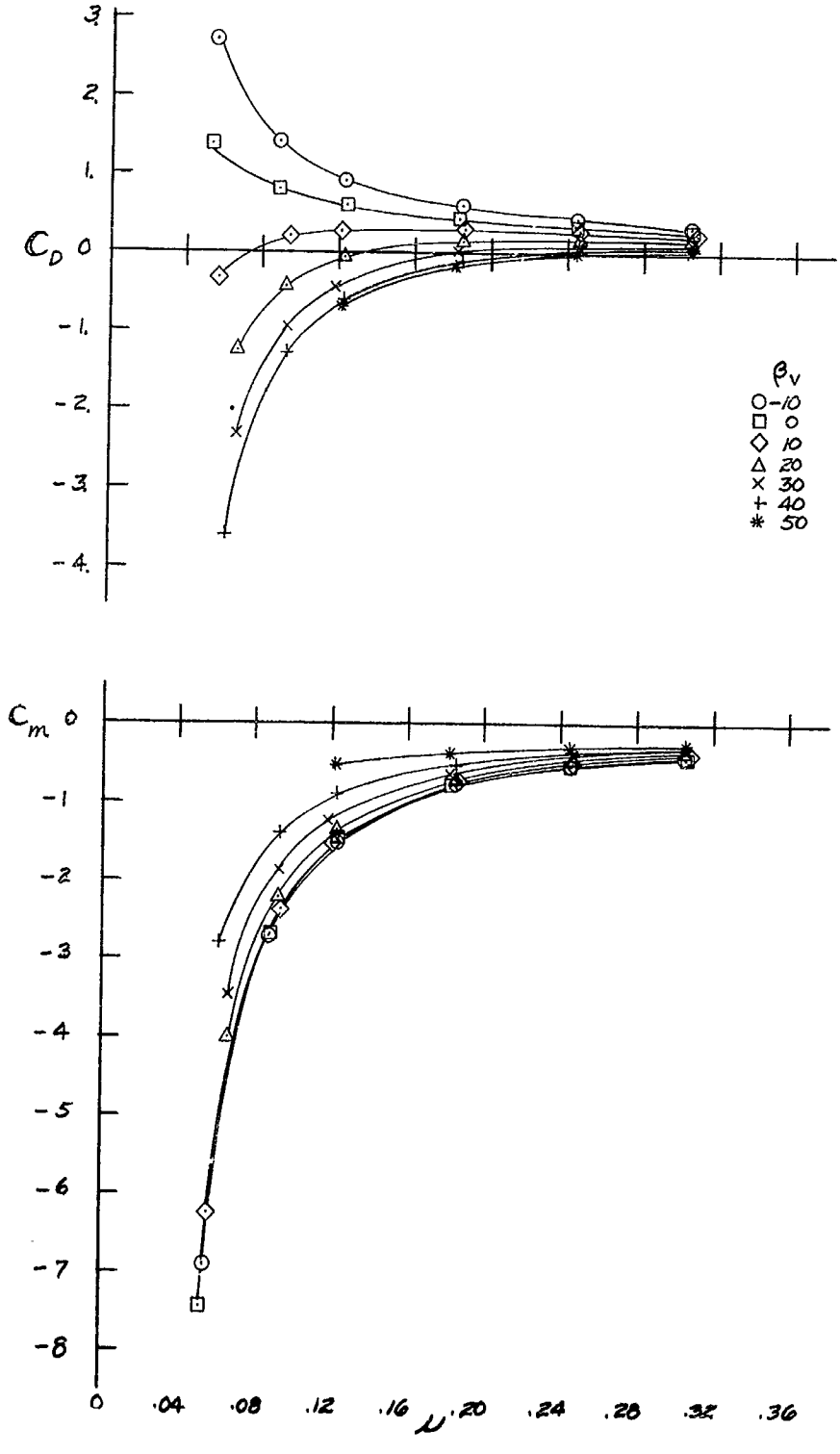

(b) C_D, C_m vs μ.

Figure 12.- Concluded.

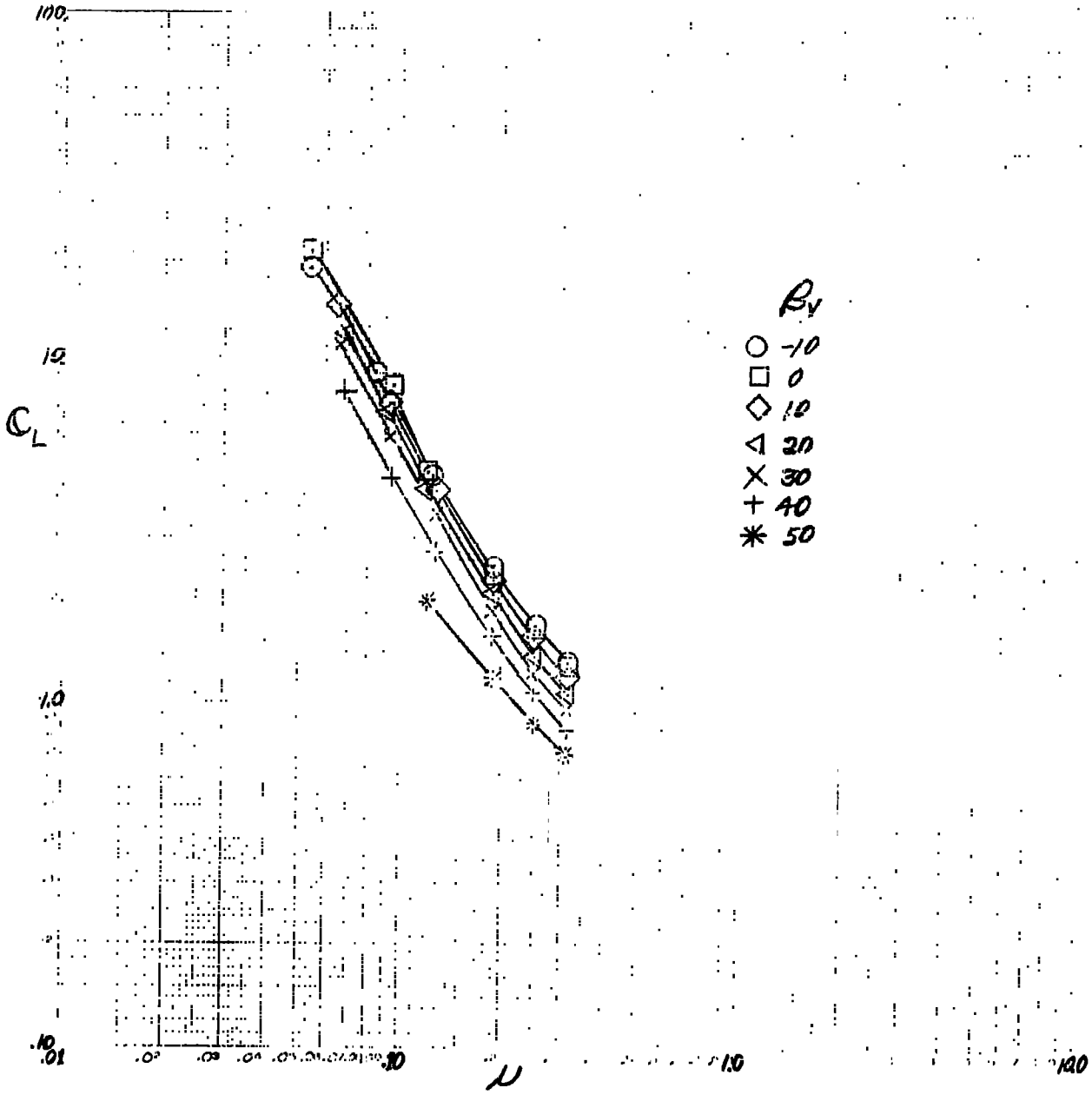

(a) C_L vs μ.

Figure 13.- The effect of tip speed ratio on longitudinal characteristics; 4 fans operating, RPM = 3300, tail off, $\delta_f = 45^o$, $\delta f_{aux} = 45^o$.

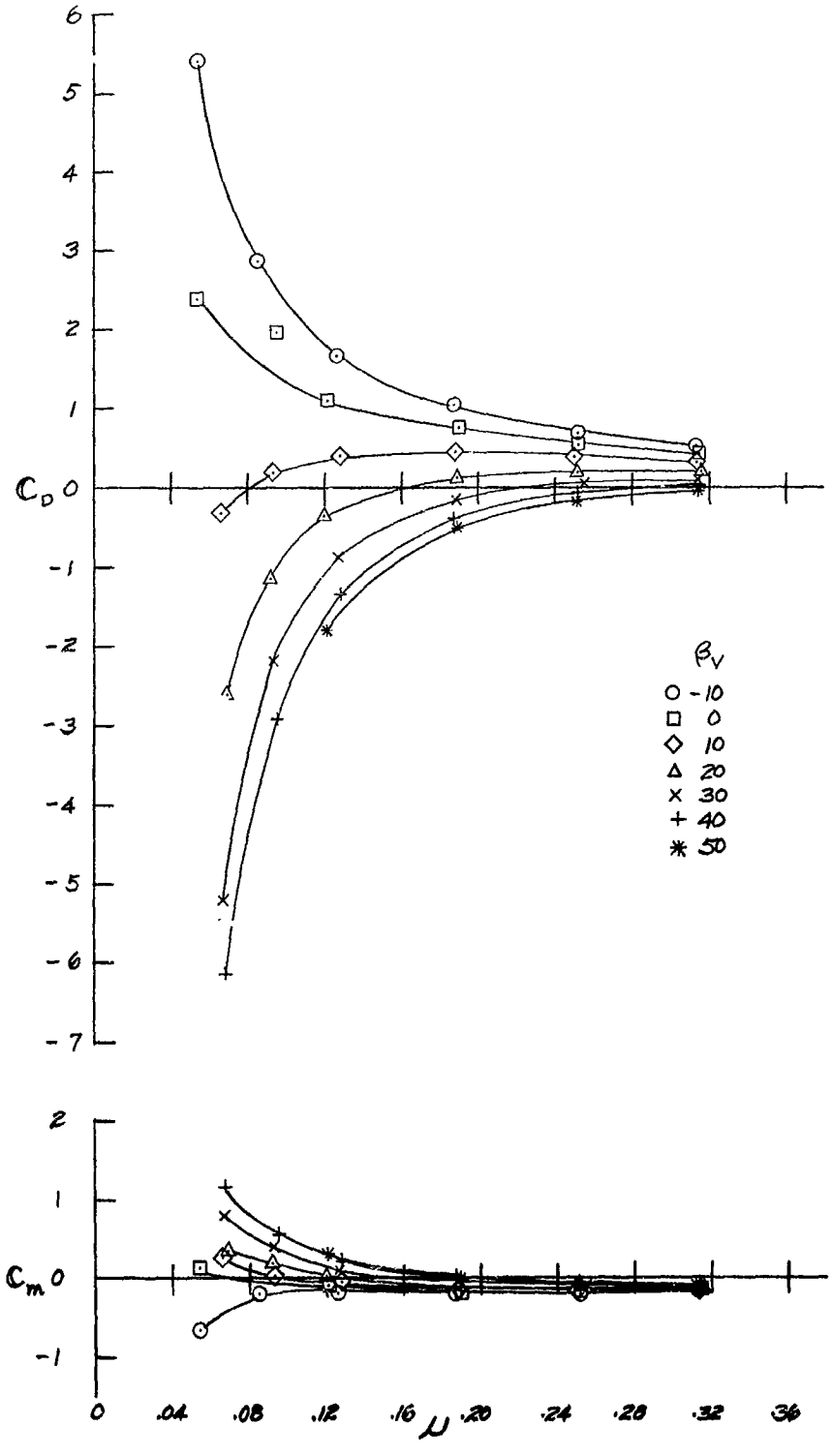

(b) C_D, C_m vs μ.

Figure 13.- Concluded.

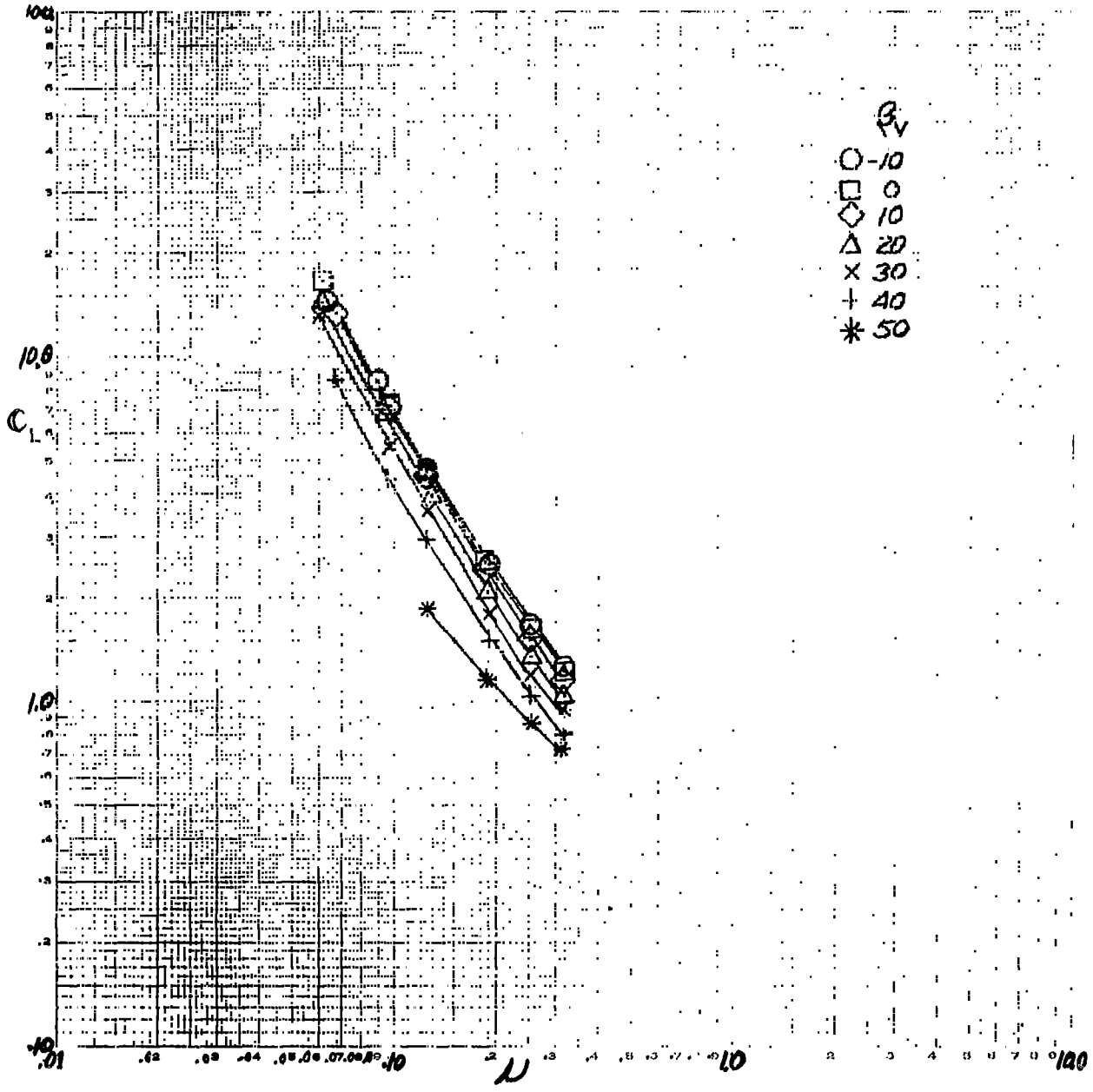

(a) C_L vs μ.

Figure 14.- The effect of tip speed ratio on longitudinal characteristics; 4 fans operating, RPM = 3300, tail off, $\delta_f = 45^o$, $\delta_{f_{aux}} = 45^o$, inlet guide vane on front fans.

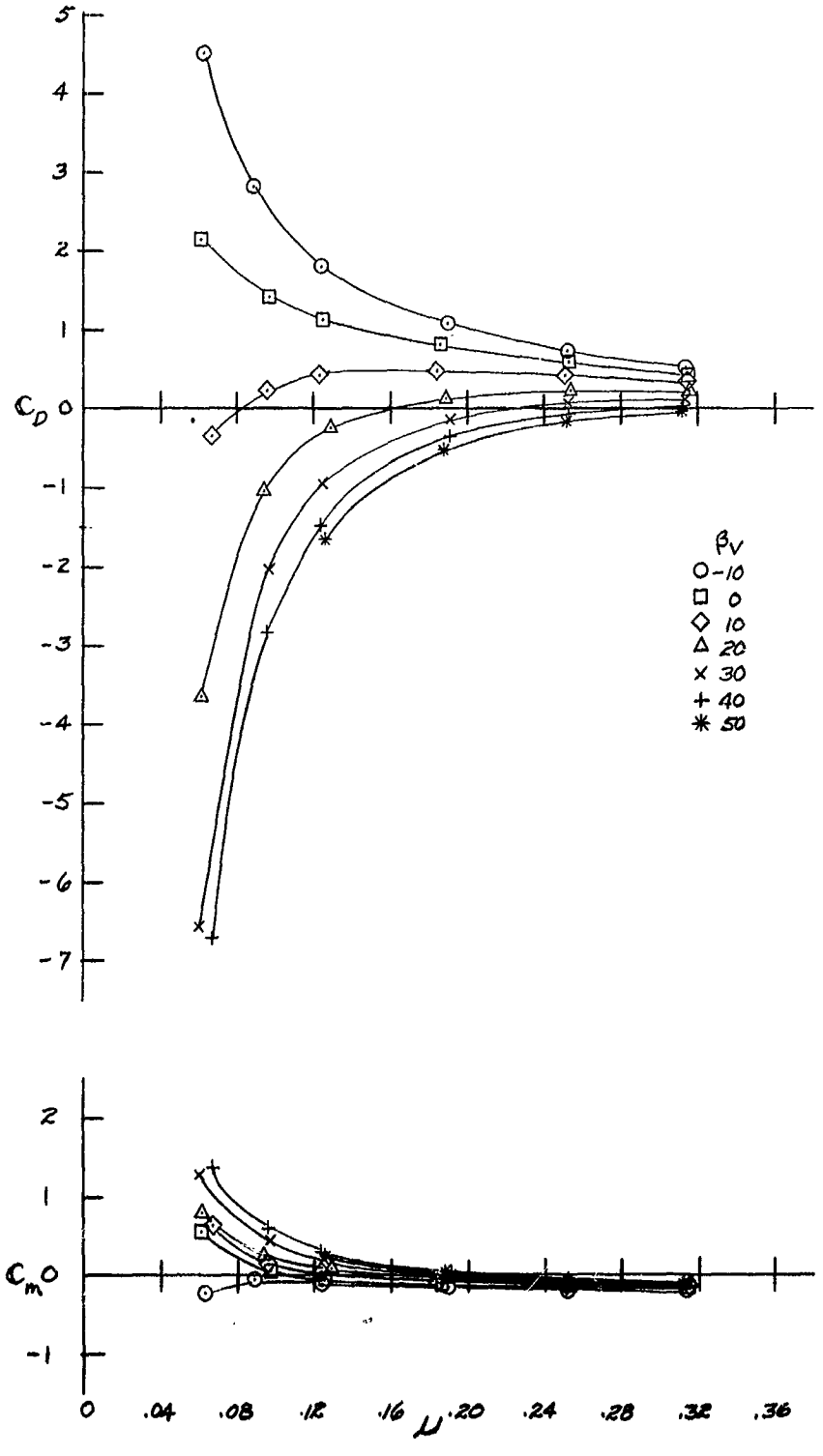

(b) C_D, C_m vs μ.

Figure 14.- Concluded.

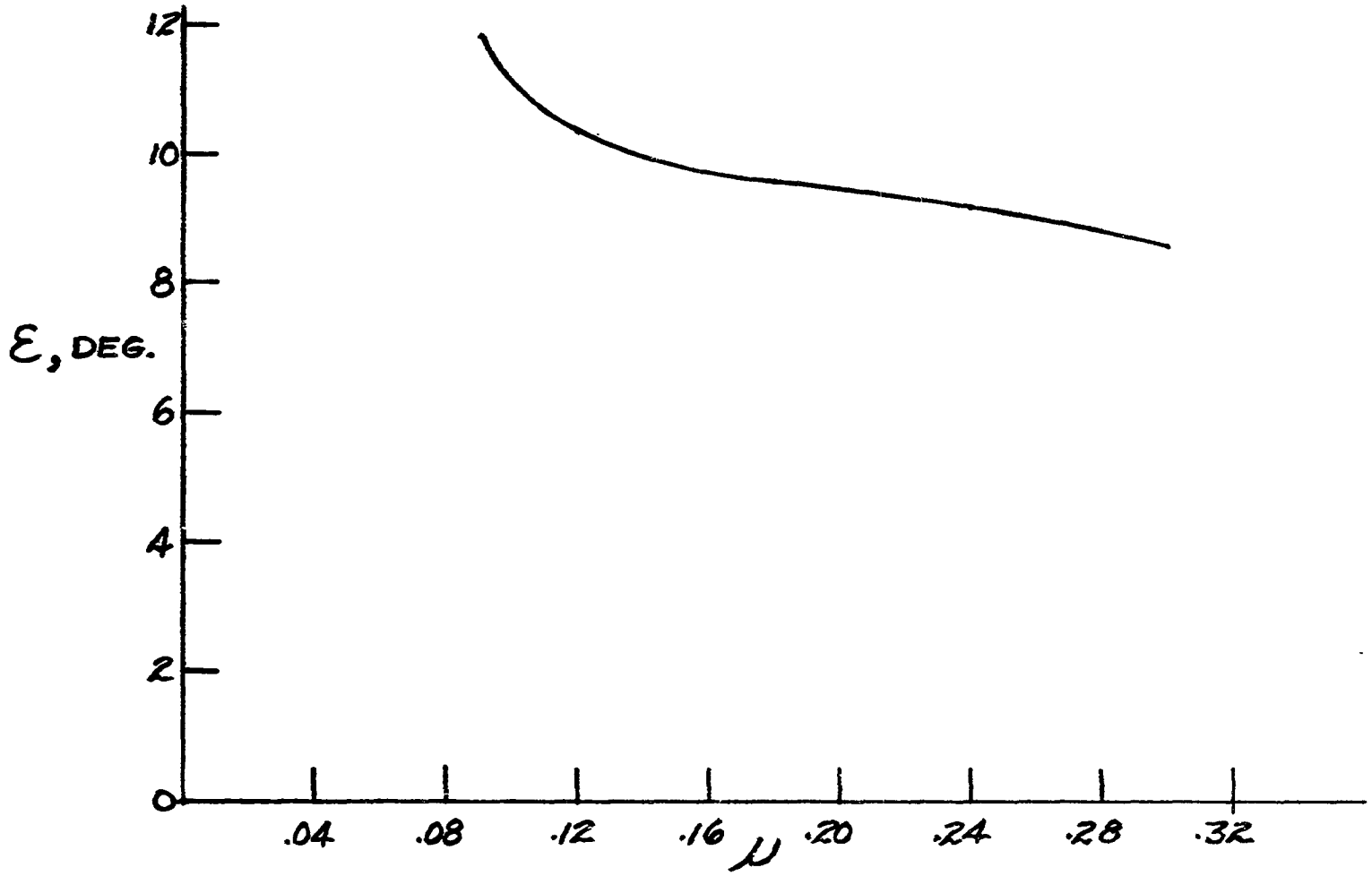

Figure 15.- Average downwash at the horizontal tail with tip speed ratio; all 4 fans operating at 3300 RPM, $\alpha = 0^{o}$, $\delta_f = 45^{o}$, $\beta_v = 0^{o}$.

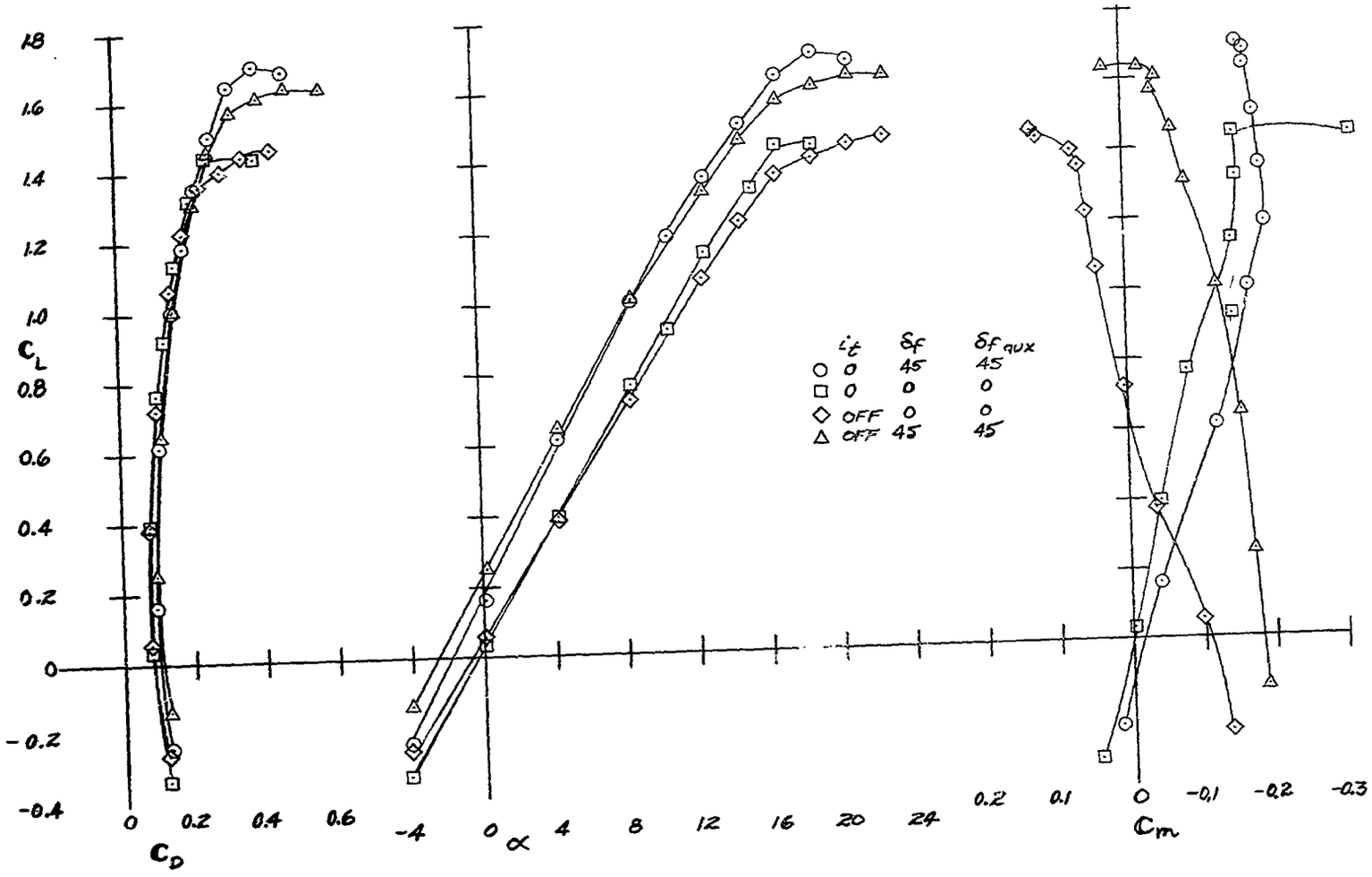

Figure 16.- Longitudinal characteristics with power off; fans sealed, $\beta_v = 90^o$, V_o = 41.2 m/sec (80 knots).

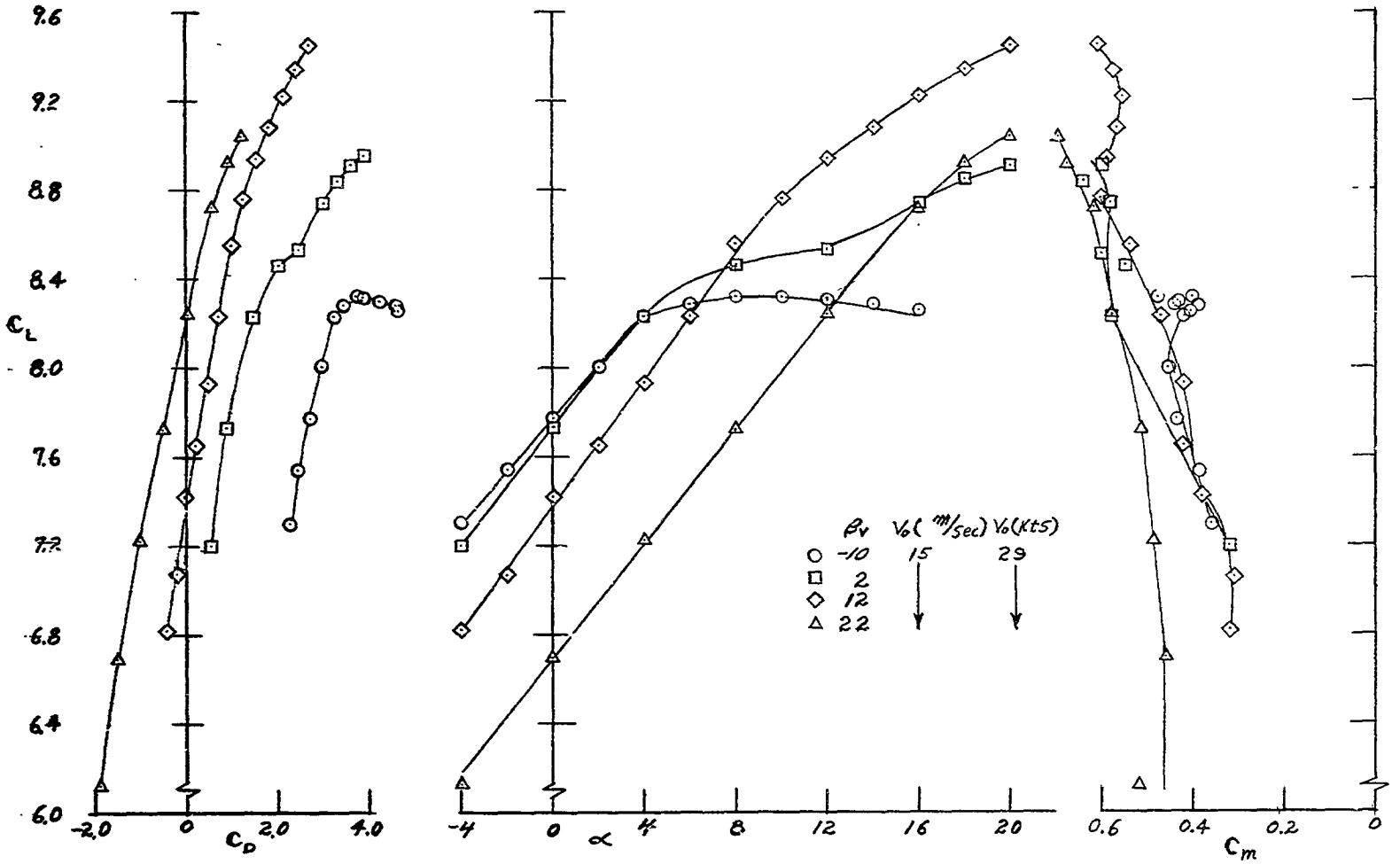

(a) $\mu_{avg.} = 0.09$.

Figure 17.- Longitudinal characteristics with fan operation; 4 fans, RPM = 3300, tail on, $i_t = 0^o$, $\delta_f = 45^o$, $\delta_{f_{aux}} = 45^o$.

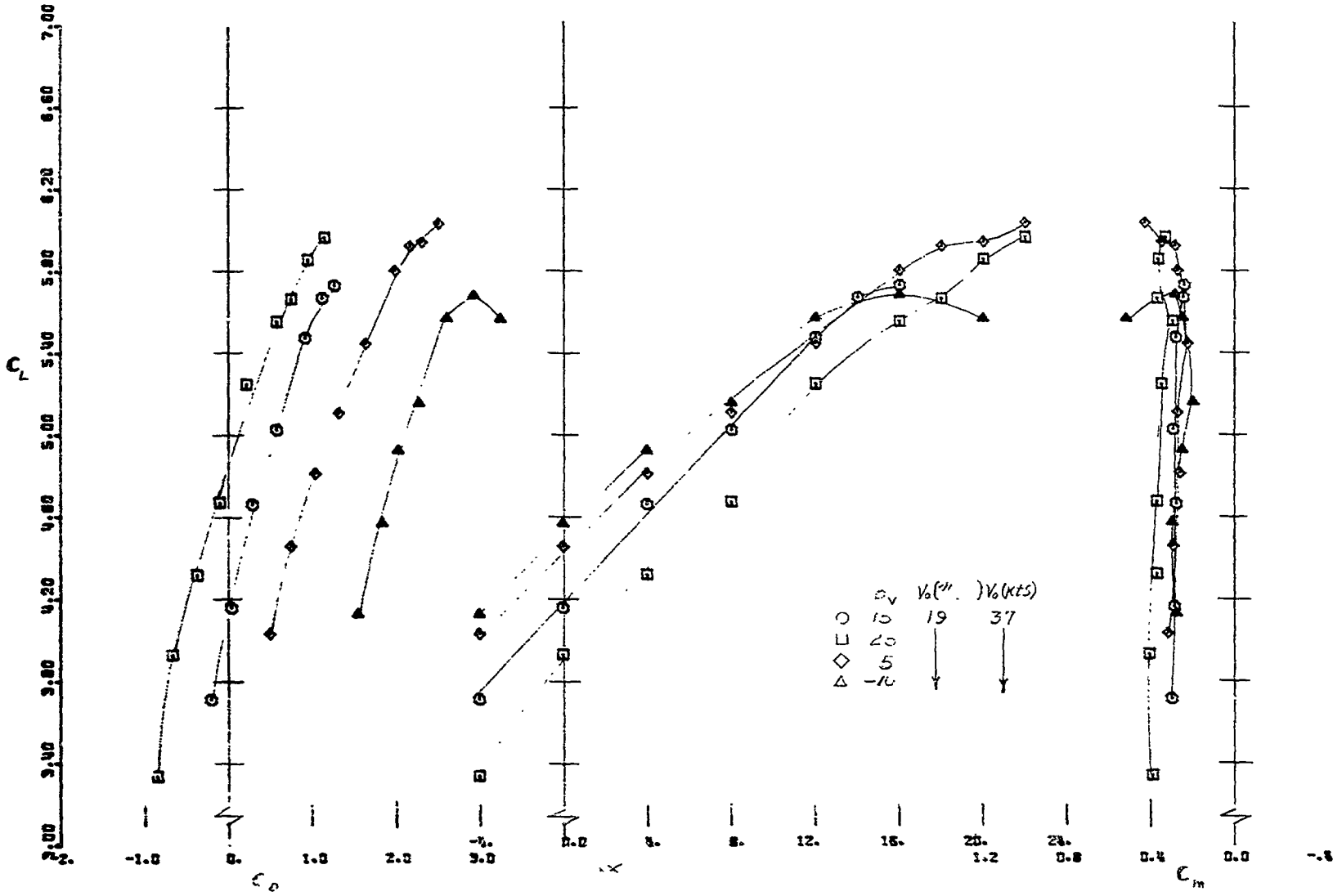

(b) $\mu_{avg.} = 0.12.$

Figure 17.- Continued.

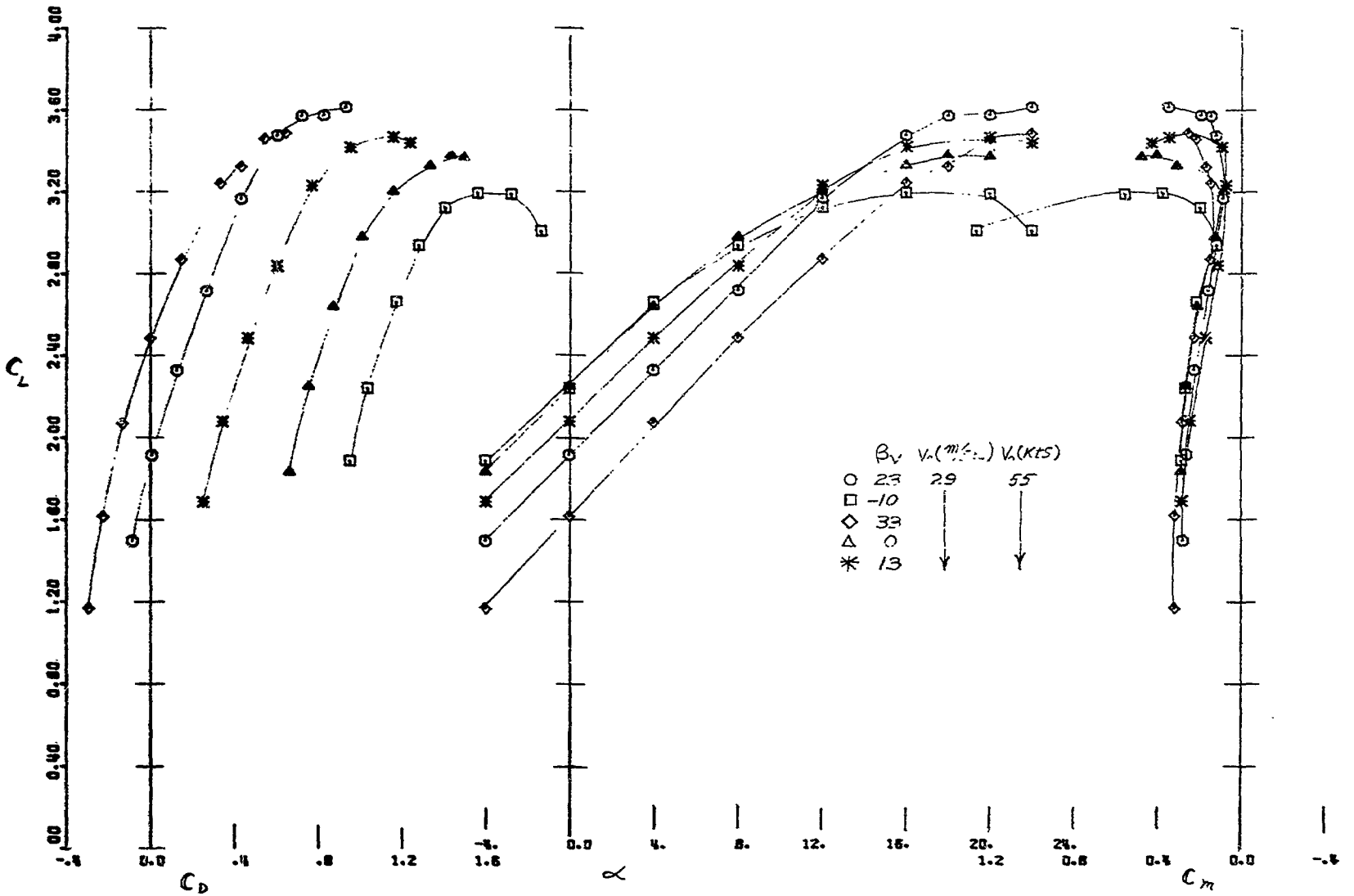

(c) $\mu_{avg.} = 0.19.$

Figure 17.- Continued.

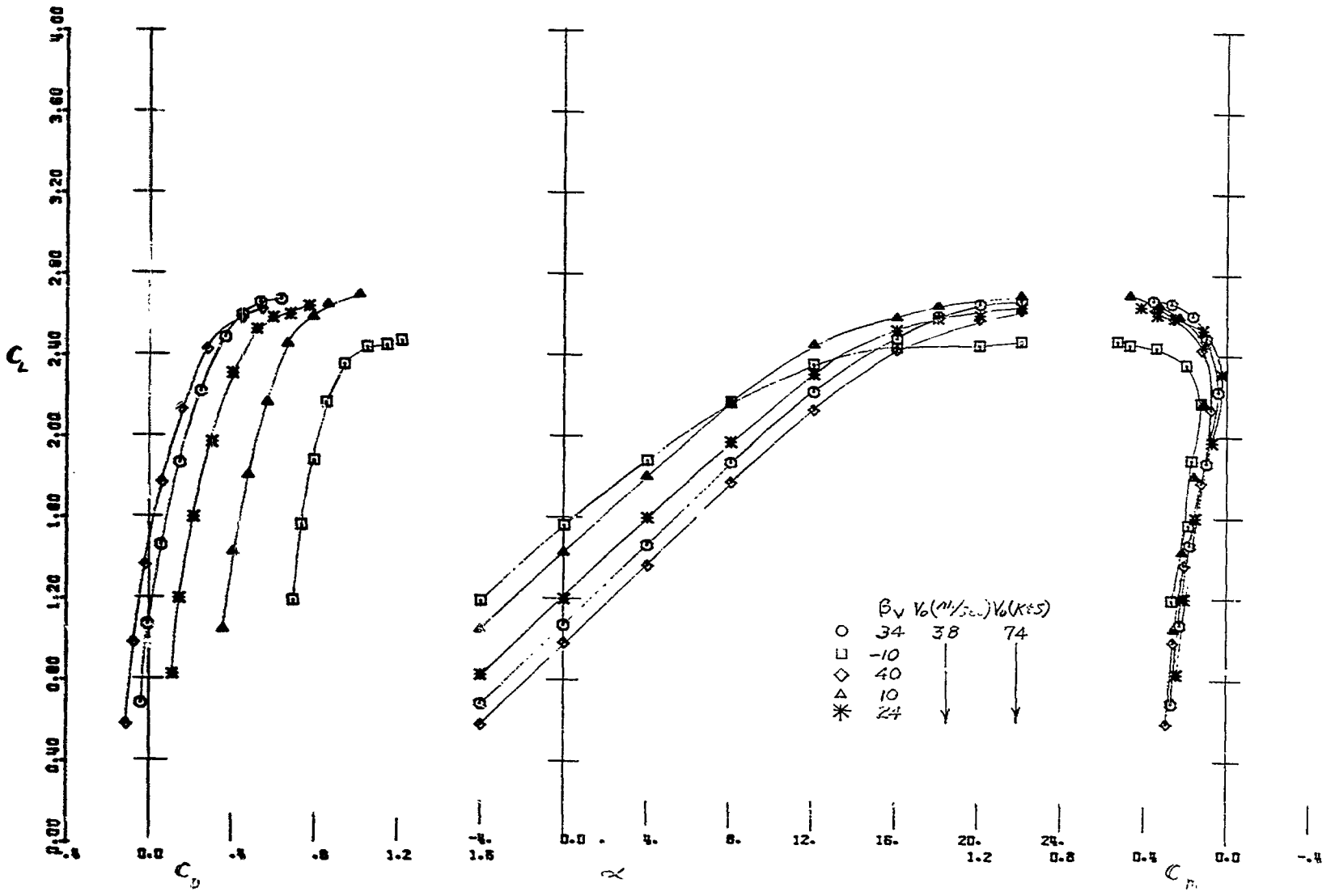

(d) $\mu_{avg.} = 0.24$.

Figure 17.- Continued.

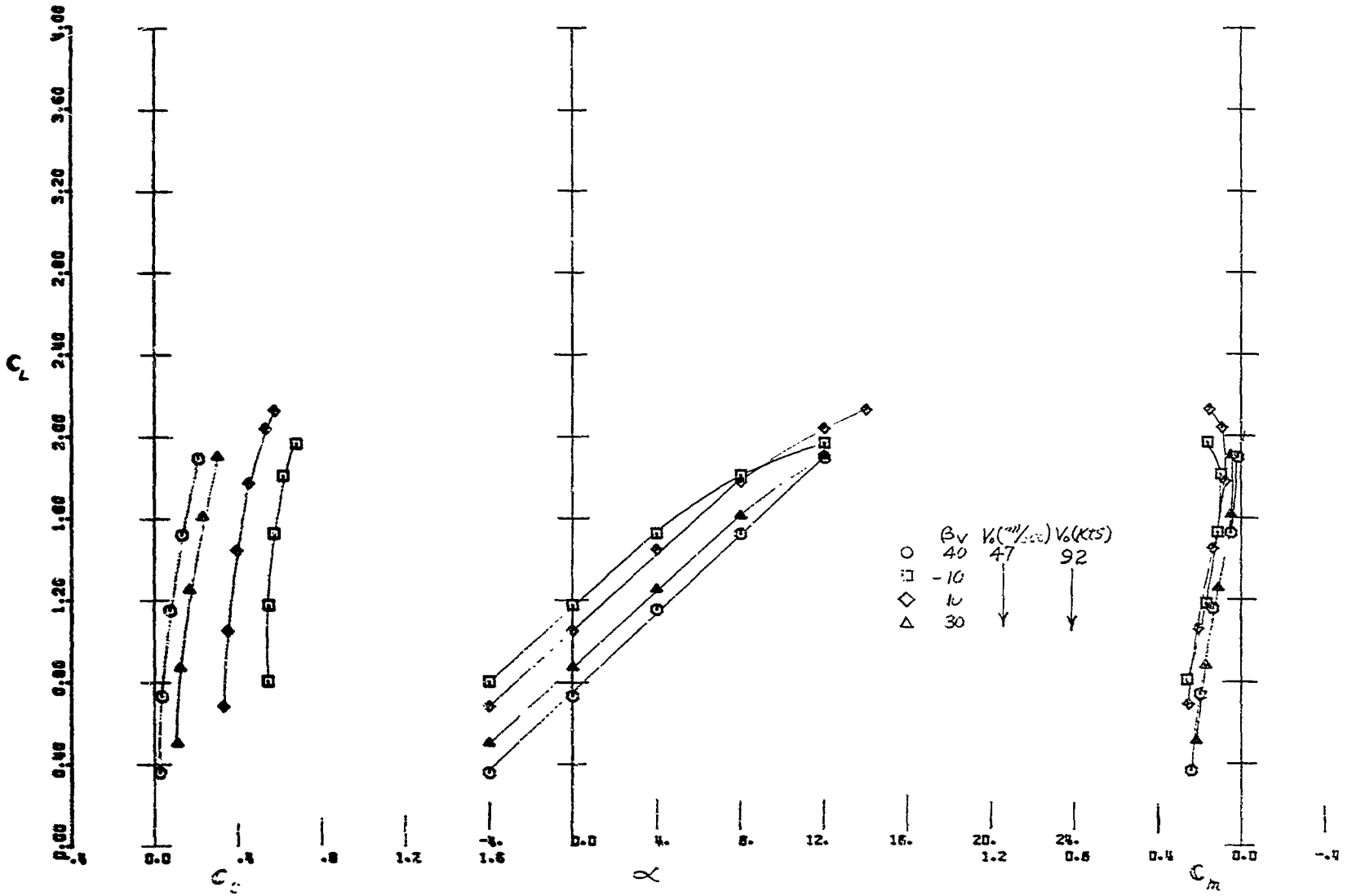

(e) $\mu_{avg.} = 0.31.$

Figure 17.- Concluded.

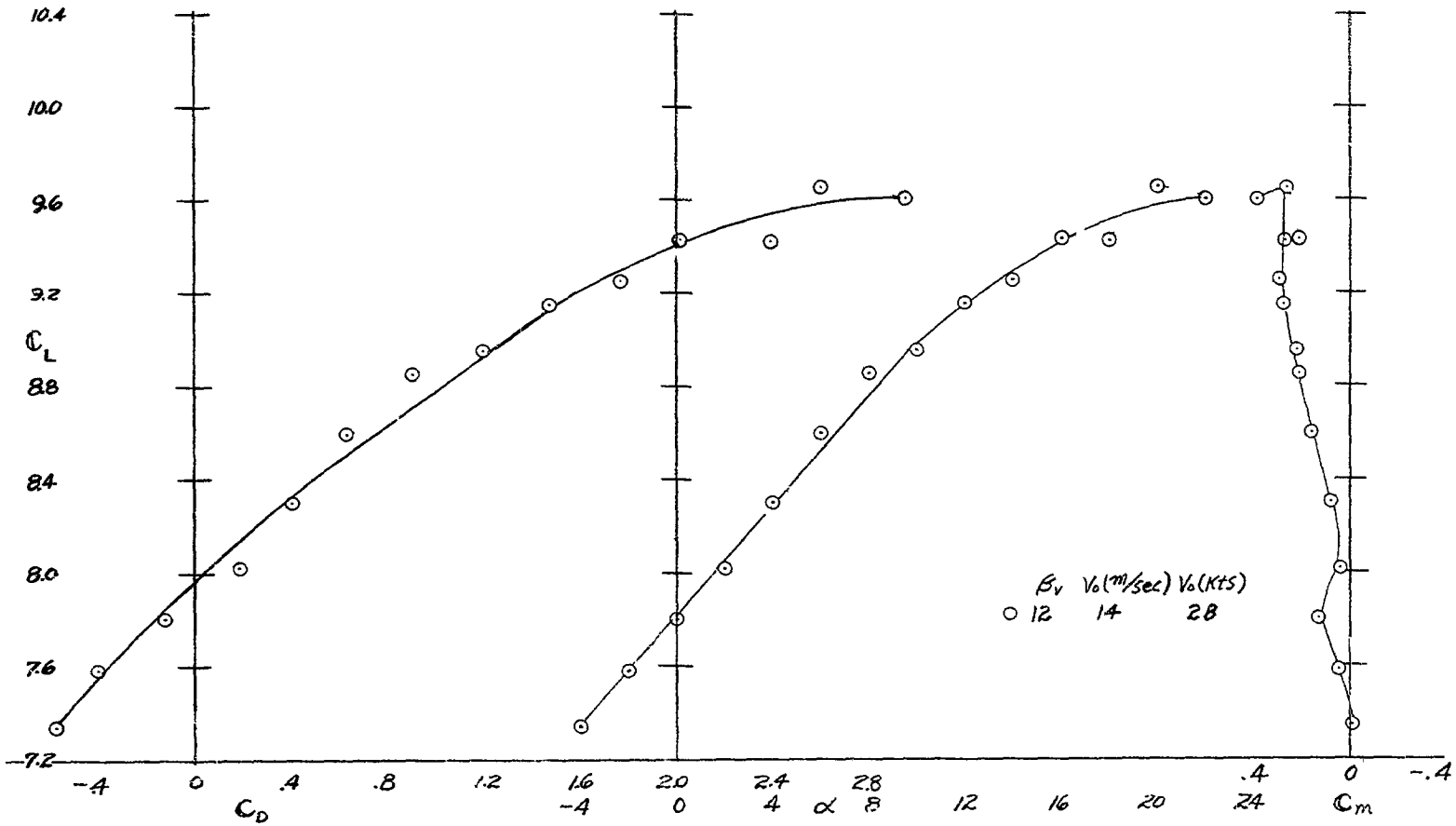

(a) $\mu_{avg.} = 0.09$.

Figure 18.- Longitudinal characteristics with fan operation; 4 fans, RPM = 3300, tail off, $\delta_f = 45^o$, $\delta_{f_{aux}} = 45^o$.

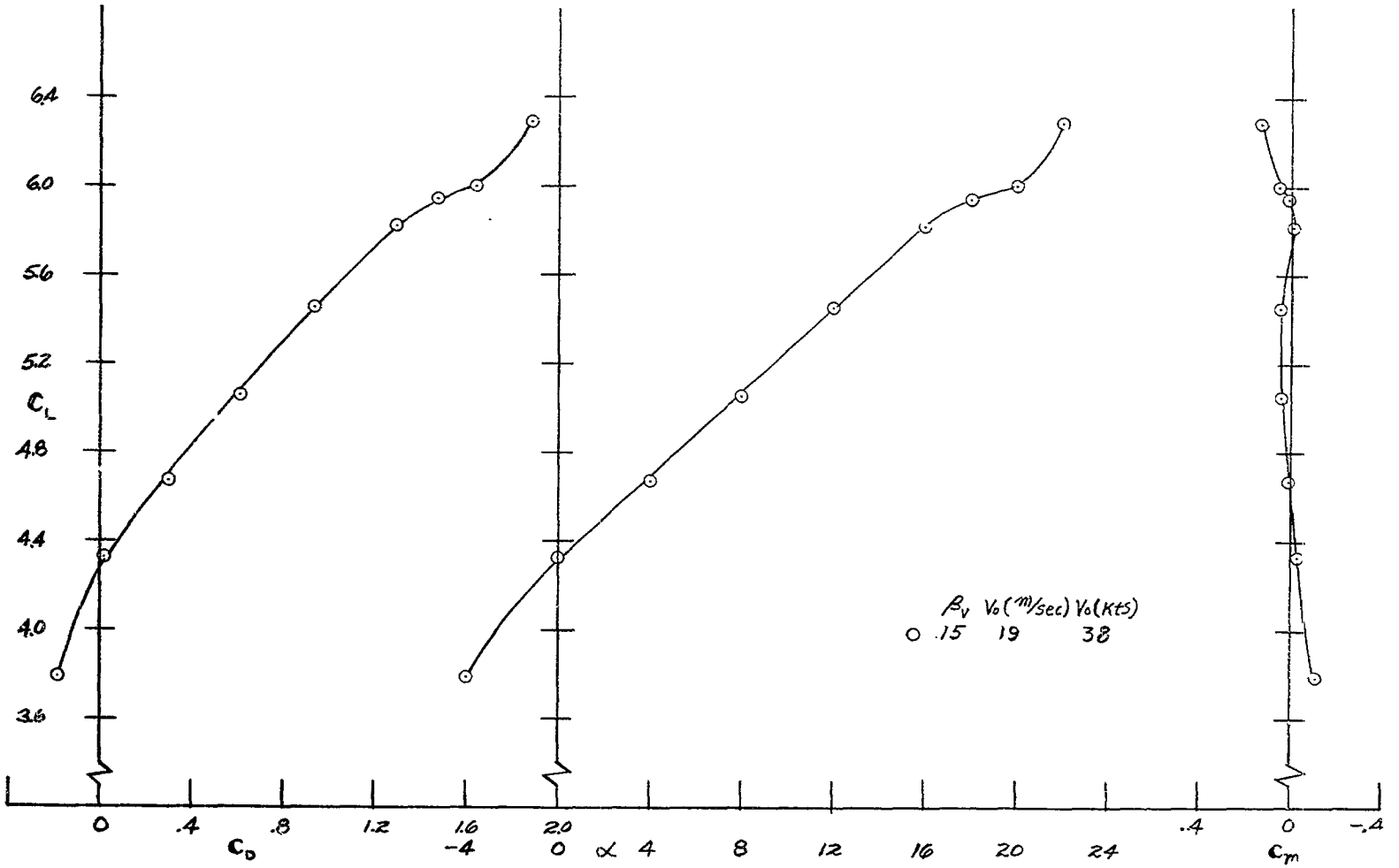

(b) $\mu_{avg.} = 0.13$.

Figure 18.- Continued.

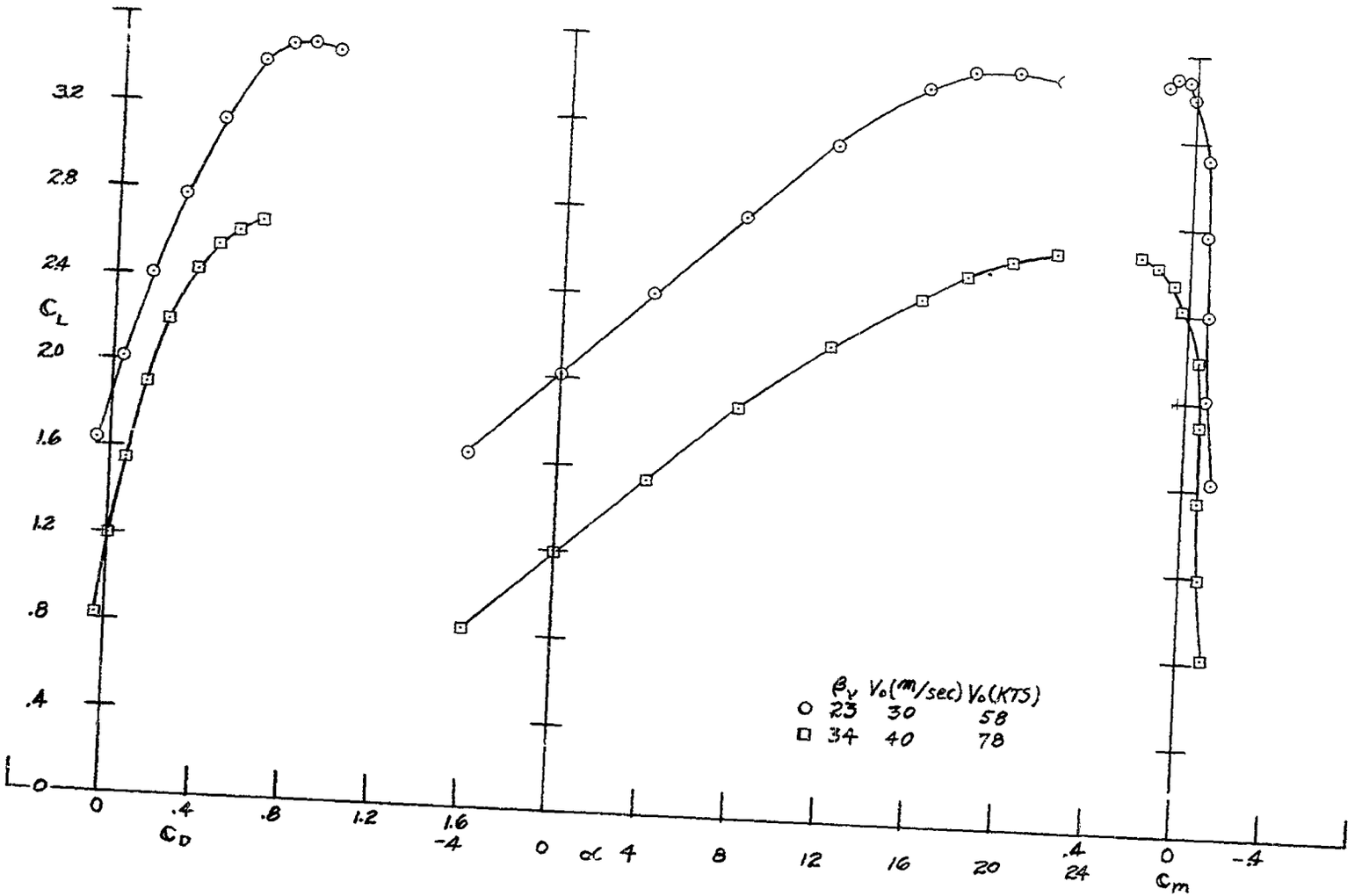

(c) $\mu_{avg.}$ = 0.19 and 0.25.

Figure 18.- Concluded.

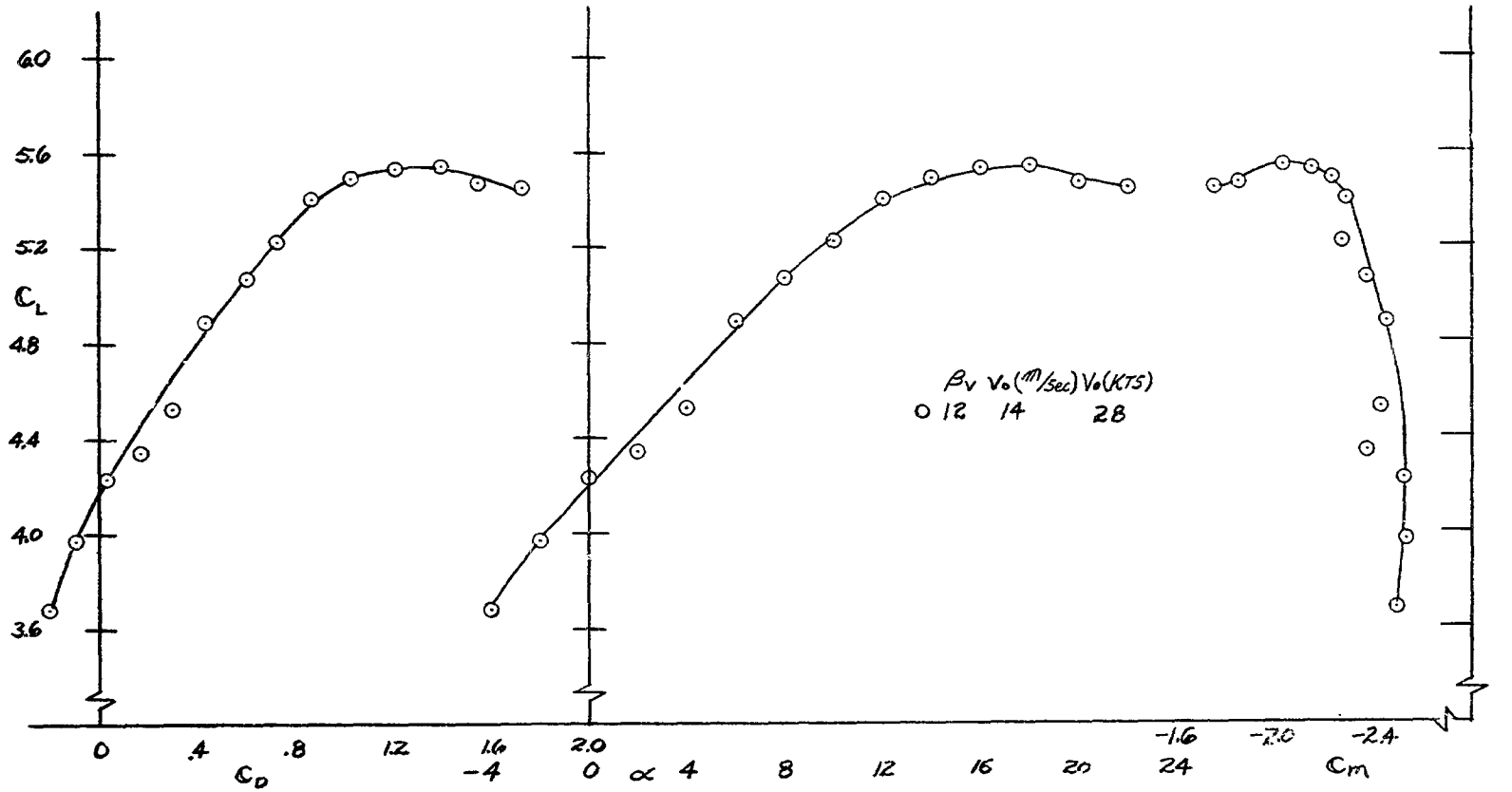

(a) $\mu_{avg.} = 0.09$.

Figure 19.- Longitudinal characteristics with fan operation; 4 fans, RPM = 3300, tail off, $\delta_f = 45^o$, $\delta_{f_{aux}} = 45^o$.

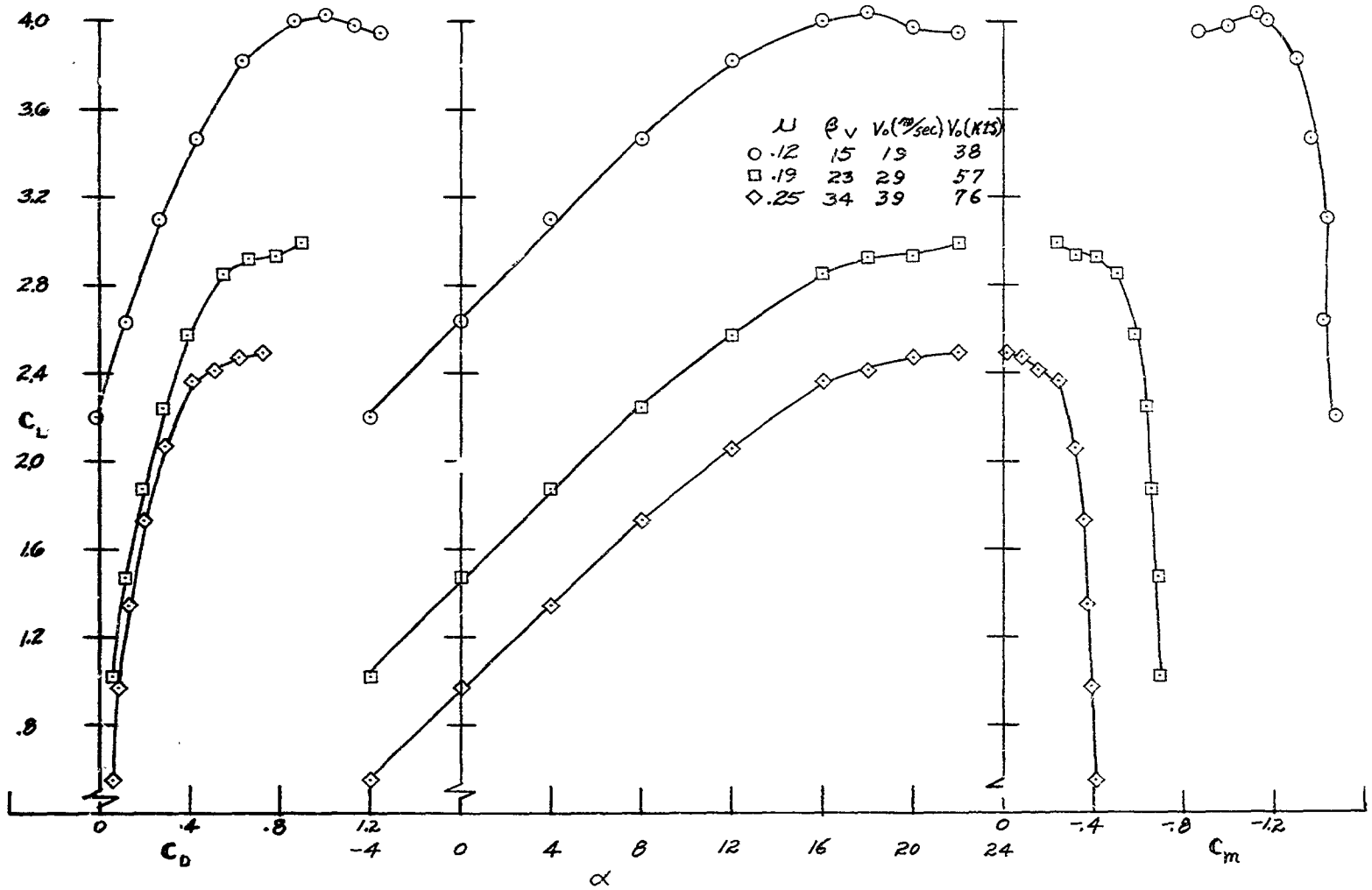

(b) $\mu_{avg.}$ = 0.12, 0.19 and 0.25.

Figure 19.- Concluded.

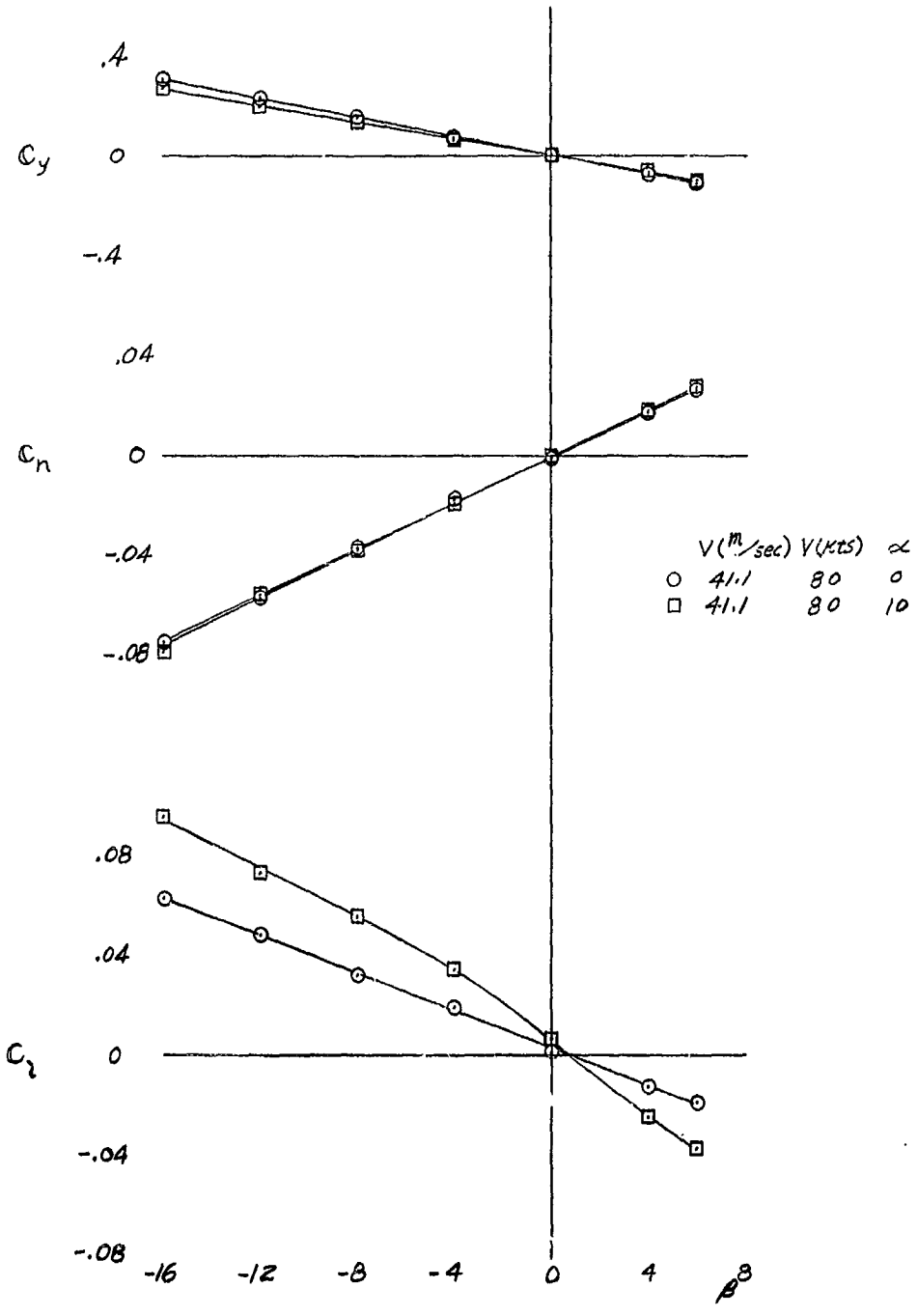

(a) Power off, $\beta_v = 50^o$.

Figure 20.- Lateral directional characteristics; tail on, $i_t = 0^o$, $\delta_f = 45^o$, $\delta f_{aux} = 45^o$.

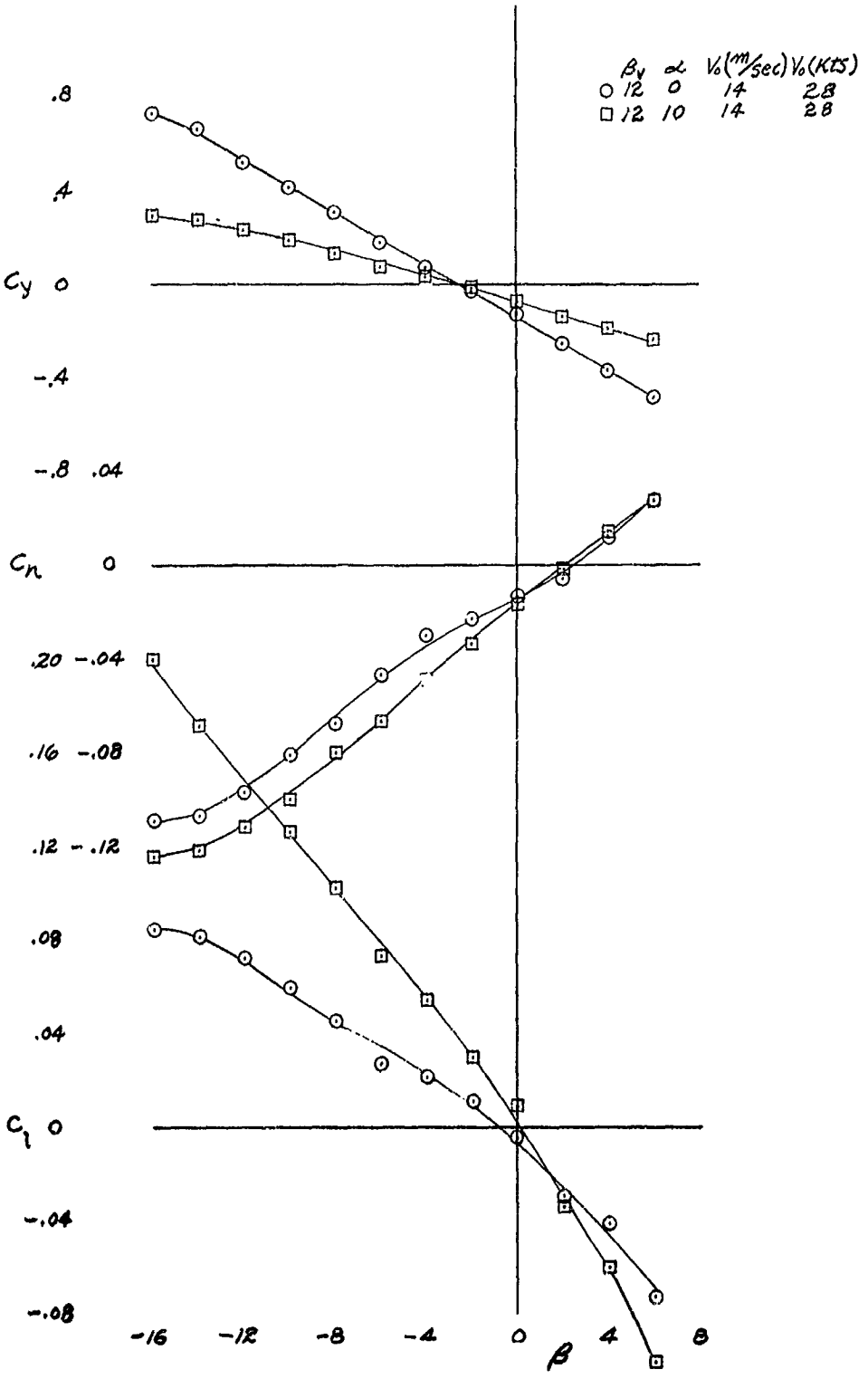

(b) $\mu_{avg.}$ = 0.09, four fans operating.

Figure 20.- Continued.

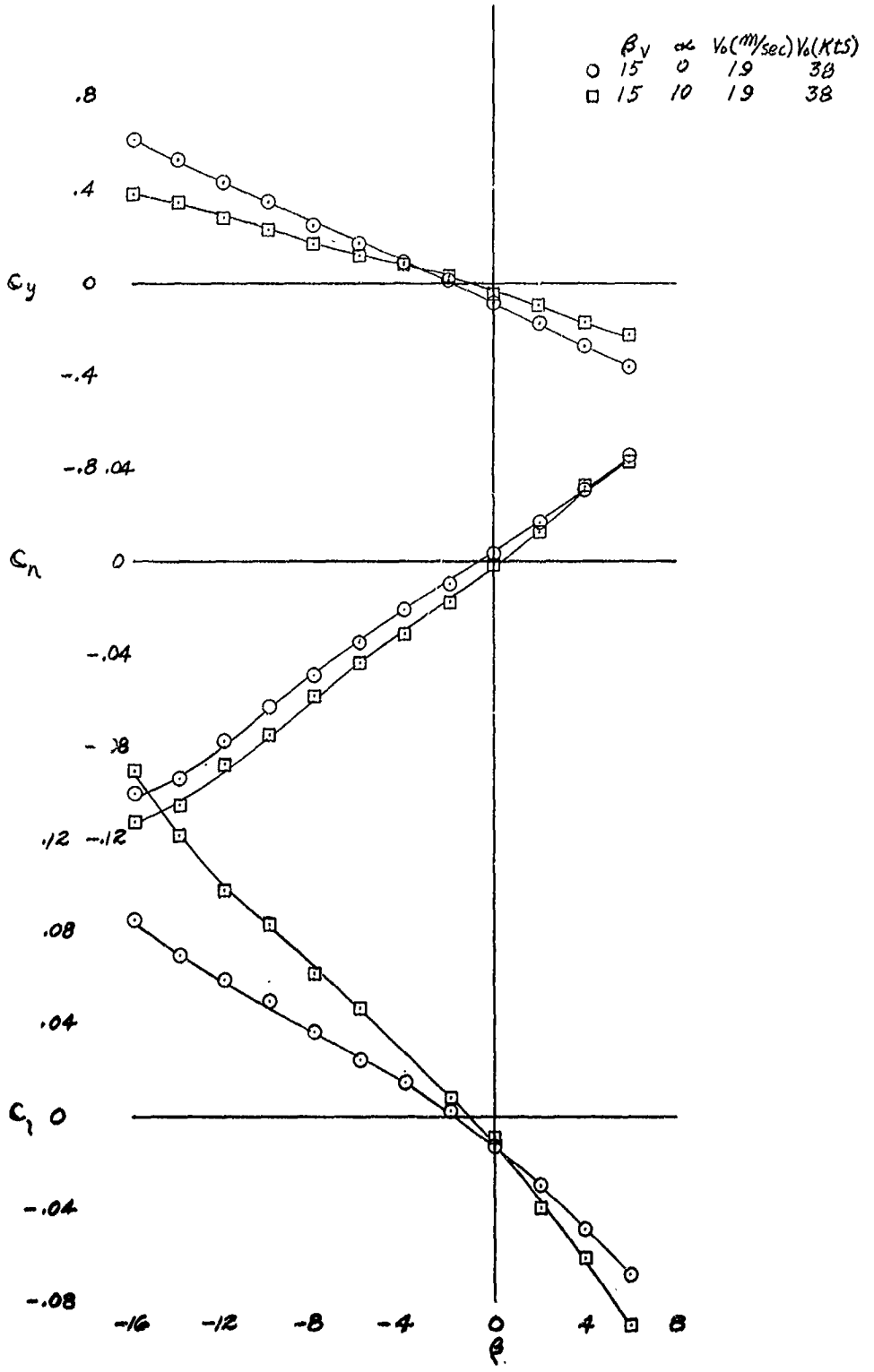

(c) $\mu_{avg.} = 0.12$.

Figure 20.- Continued.

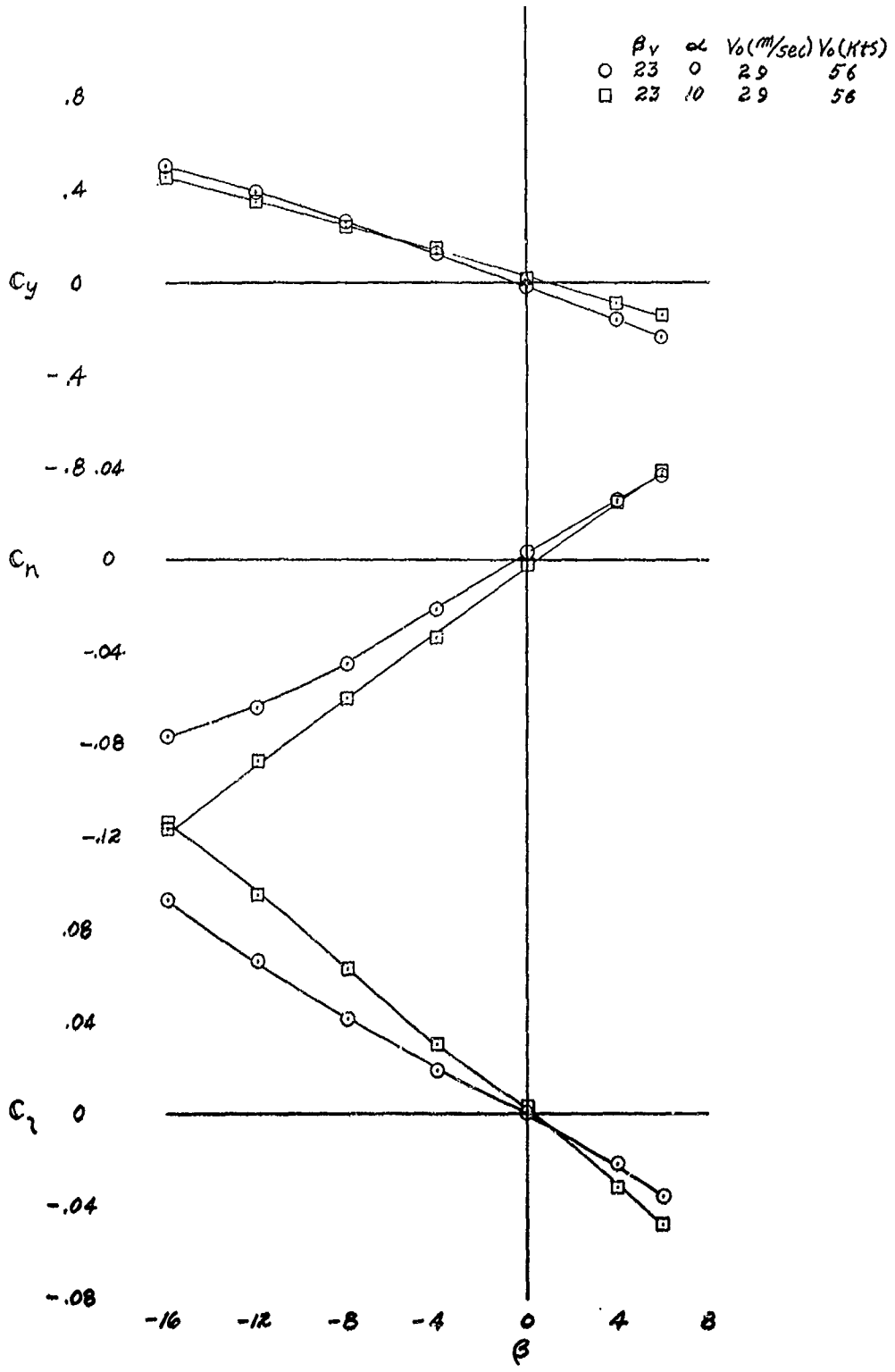

(d) $\mu_{avg.} = 0.19$.

Figure 20.- Continued.

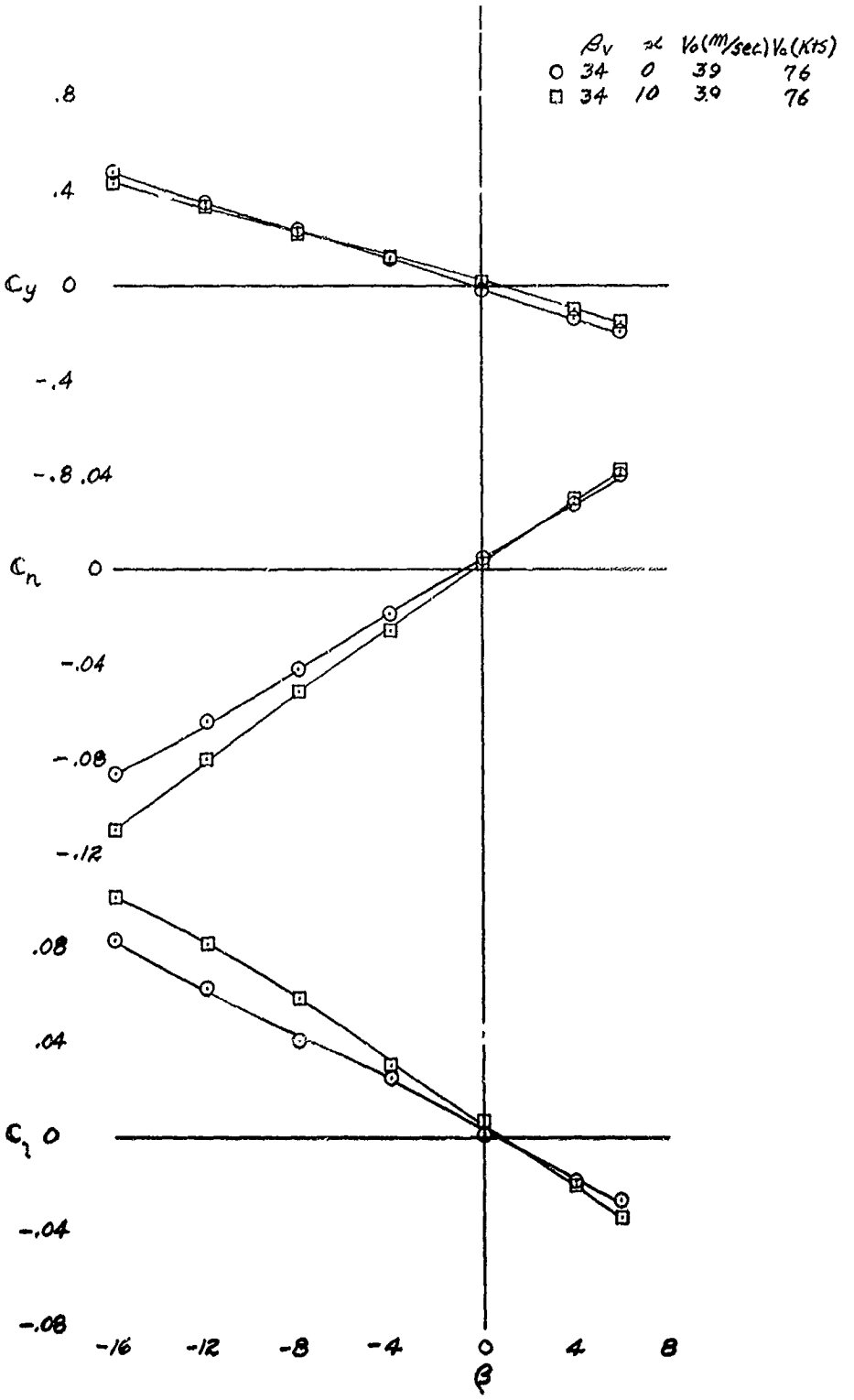

(e) $\mu_{avg.} = 0.25$.

Figure 20.- Continued.

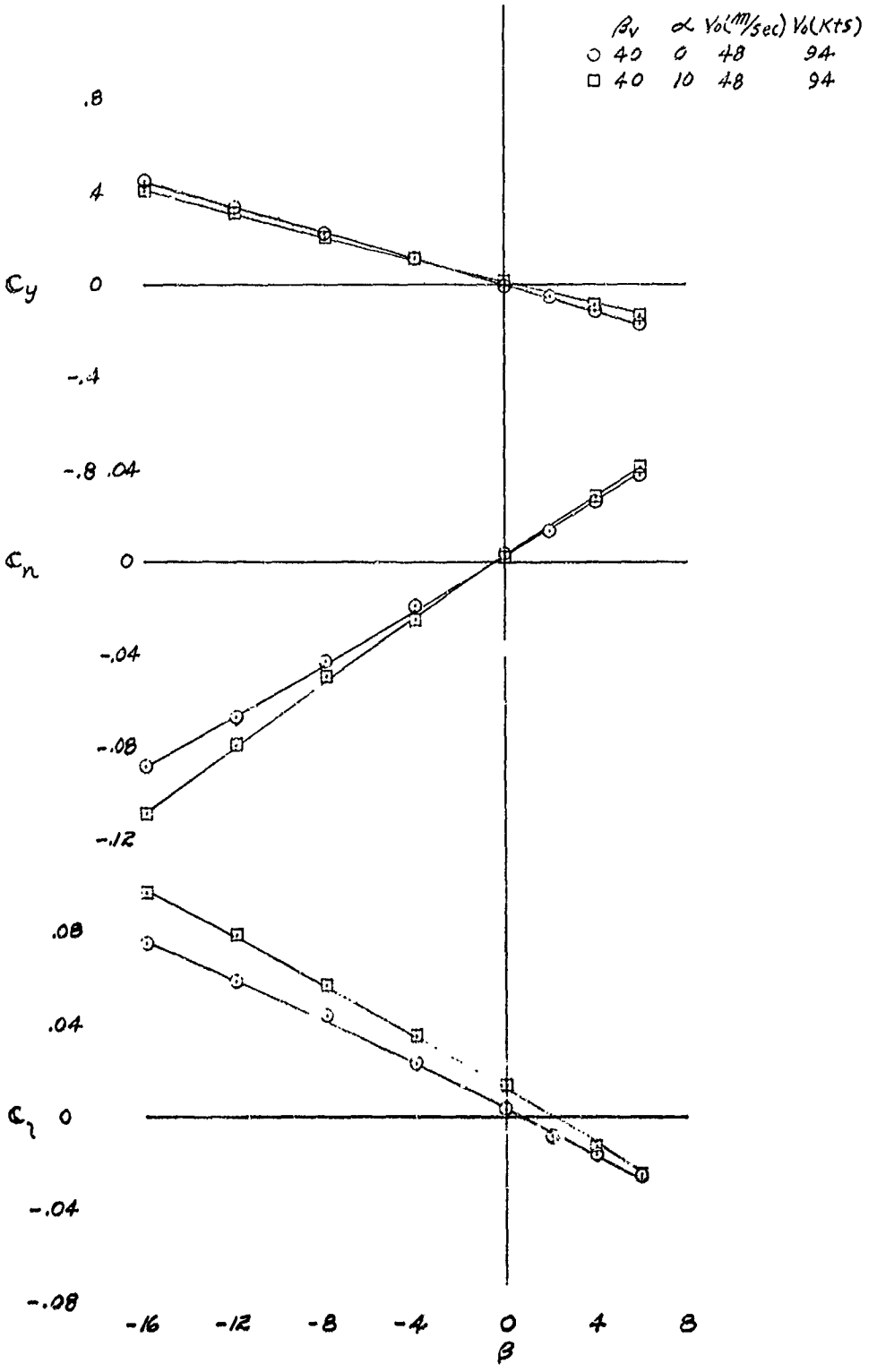

(f) $\mu_{avg.} = 0.31$.

Figure 20.- Concluded.

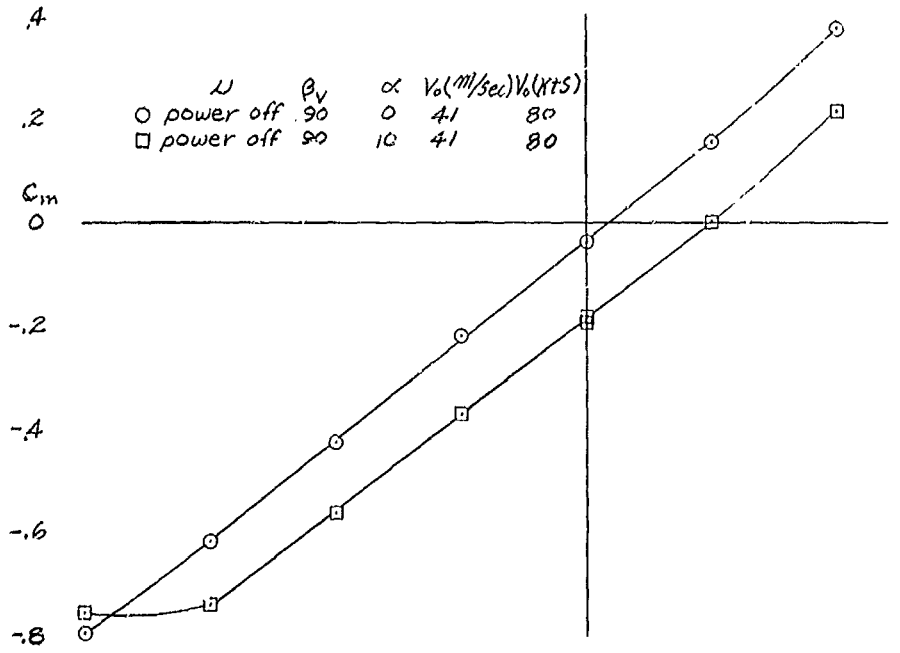

(a) Power off.

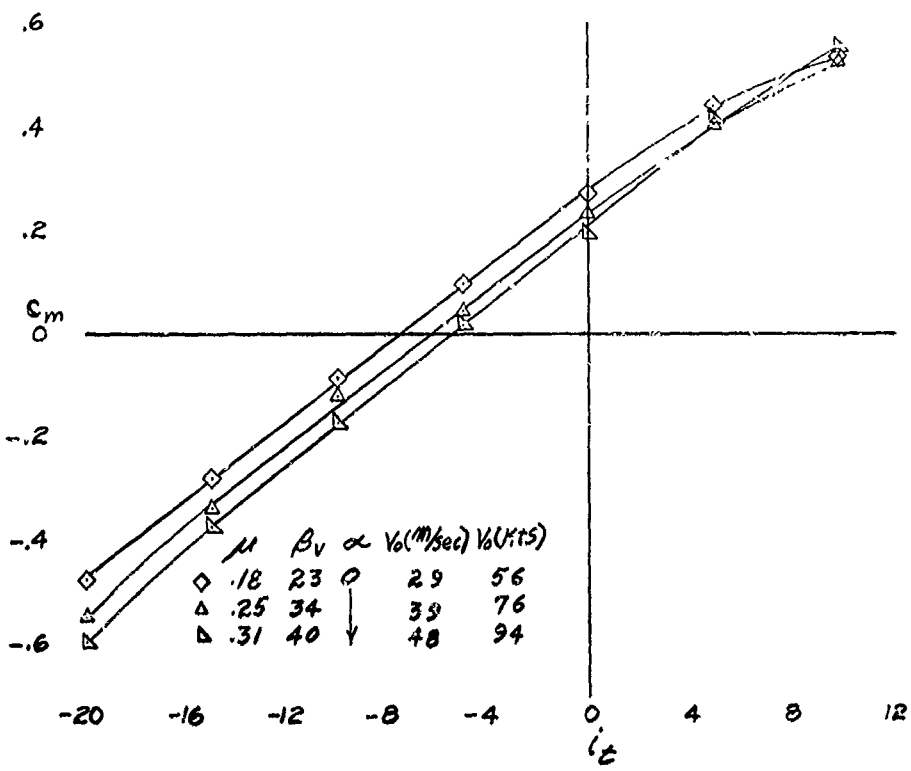

(b) Four fans operating.

Figure 21.- Effectiveness of the horizontal tail; $\delta_f = 45^\circ$, $\delta_{f_{aux}} = 45^\circ$.

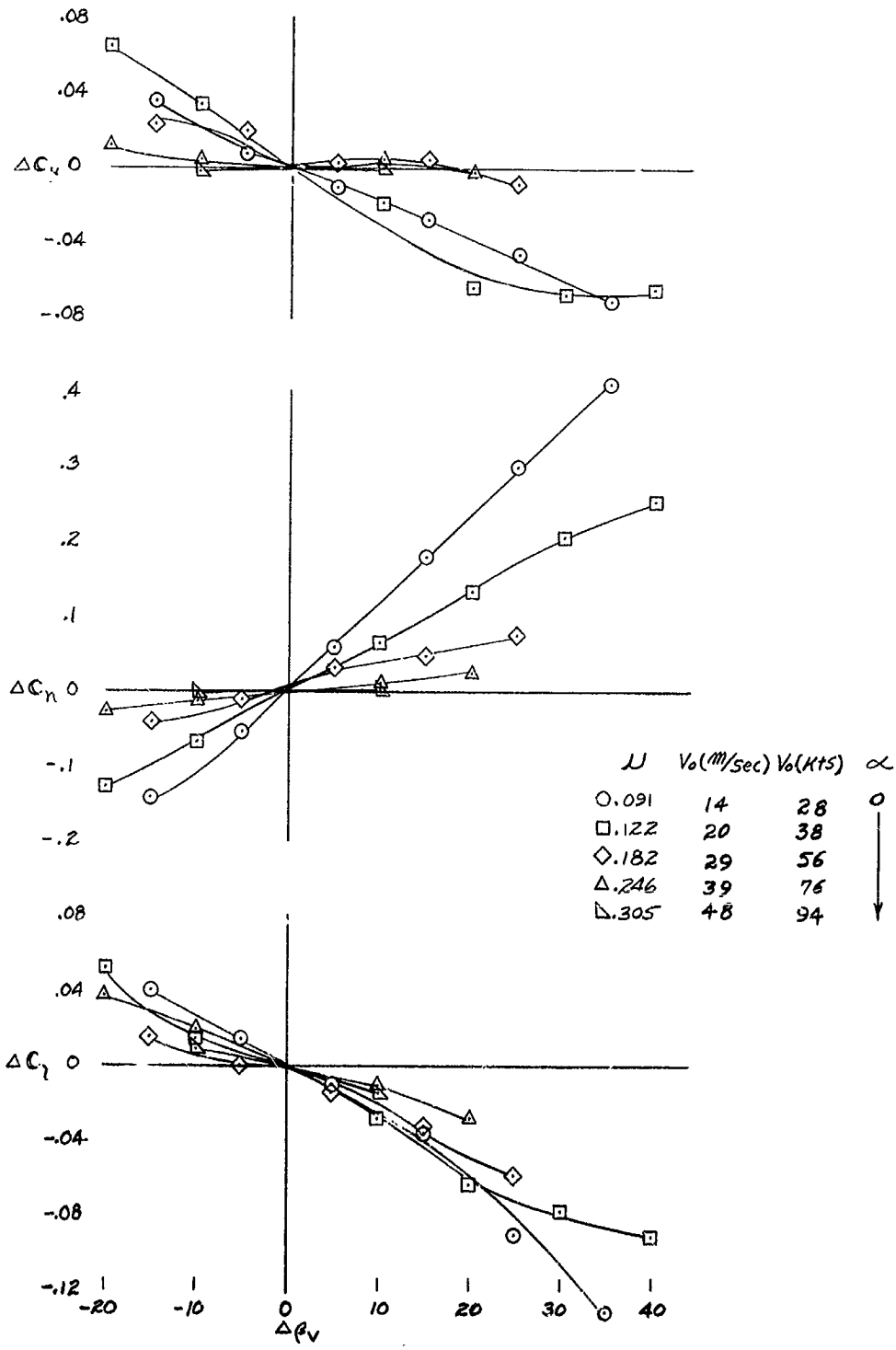

Figure 22.- The effect of using differential exit vane deflection between the left and right fans for directional control; 4 fans, RPM = 3300, tail on, $i_t = 0^o$, $\delta_f = 45^o$, $\delta_{f_{aux}} = 45^o$.

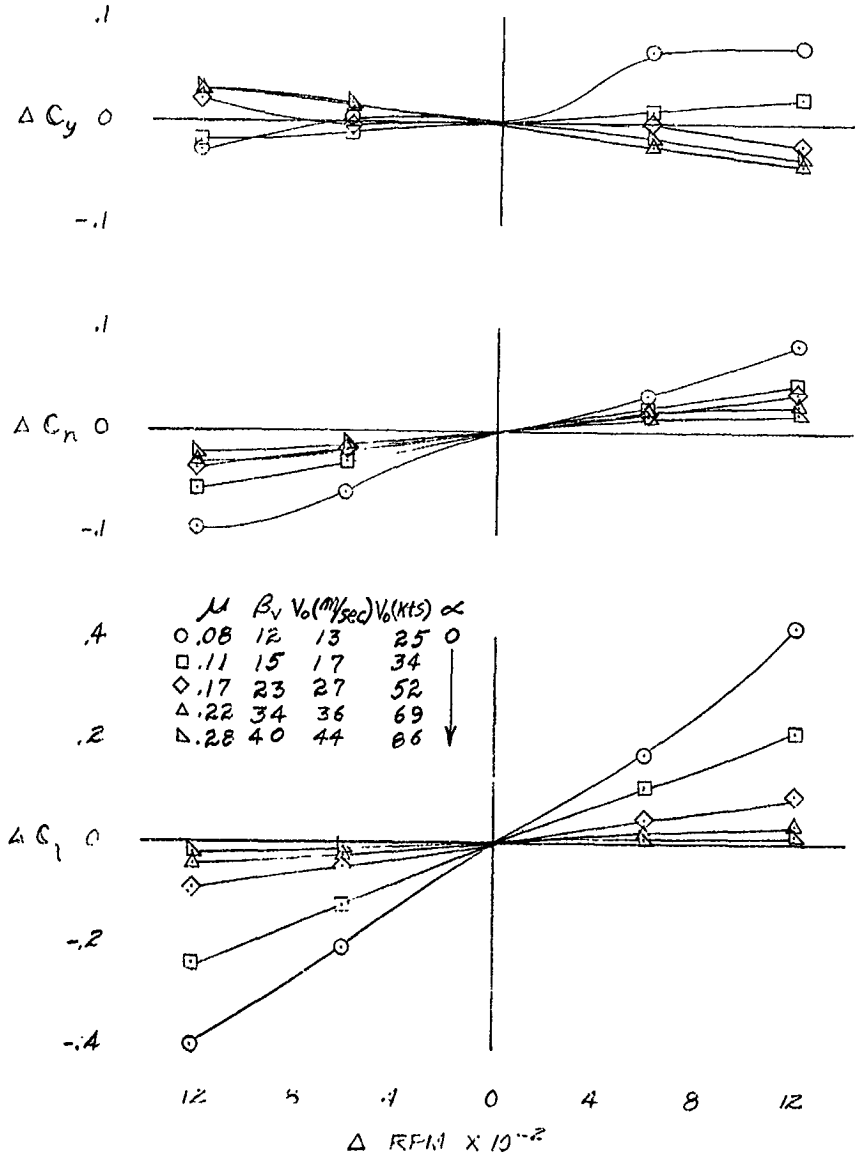

Figure 23.- The effect of using differential fan RPM between the left and right fans for roll control; 4 fans, RPM = 3300, tail on, $i_t = 0^o$, $\delta_f = 45^o$, $\delta_{f_{aux}} = 45^o$.